communicated by:
Lehr- und Forschungsgebiet Monitoring und verteilte Kontrolle für Energiesysteme
Univ.-Prof. Ferdinanda Ponci

Sensitivity and Cost-Benefit Analysis of State-Estimation based Voltage Control for Distribution Systems

Sensitivitäts- und Kosten-Nutzen-Analyse einer auf Zustandsschätzung basierenden Spannungsregelung für Verteilnetze

David Alejandro Pacheco Castro
Matriculation Number: 429493

Master Thesis

The present work was submitted to
RWTH Aachen University
Faculty of Electrical Engineering and Information Technology
Institute for Automation of Complex Power Systems
Univ.-Prof. Antonello Monti, Ph. D.

Supervisor: Mirko Ginocchi, M.Sc.

Marco Pau, Ph.D.

Aachen, den _____ _____

1. Prüfer

Eidesstattliche Versicherung

Ich, David Alejandro Pacheco Castro (Matrikelnummer 429493), versichere hiermit an Eides Statt, dass ich die vorliegende Masterarbeit mit dem Titel

Sensitivity and Cost-Benefit Analysis of State-Estimation based Voltage Control for Distribution Systems

selbstständig und ohne unzulässige fremde Hilfe erbracht habe. Ich habe keine anderen als die angegebenen Quellen und Hilfsmittel benutzt. Für den Fall, dass die Arbeit zusätzlich auf einem Datenträger eingereicht wird, erkläre ich, dass die schriftliche und die elektronische Form vollständig übereinstimmen. Die Arbeit hat in gleicher oder ähnlicher Form noch keiner Prüfungsbehörde vorgelegen.

Ort, Datum	Unterschrift

Belehrung

§156 StGB: Falsche Versicherung an Eides Statt

Wer vor einer zur Abnahme einer Versicherung an Eides Statt zuständigen Behörde eine solche Versicherung falsch abgibt oder unter Berufung auf eine solche Versicherung falsch aussagt, wird mit einer Freiheitsstrafe bis zu drei Jahren oder mit Geldstrafe bestraft.

§161 StGB: Fahrlässiger Falscheid; fahrlässige falsche Versicherung an Eides Statt

(1) Wenn eine der in den §§ 154 bis 156 bezeichneten Handlungen aus Fahrlässigkeit begangen worden ist, so tritt Freiheitsstrafe bis zu einem Jahr oder Geldstrafe ein.
(2) Straflosigkeit tritt ein, wenn der Täter die falsche Angabe rechtzeitig berichtigt. Die Vorschriften des §158 Abs. 2 und 3 gelten entsprechend.

Die vorstehende Belehrung habe ich zur Kenntnis genommen:

Ort, Datum	Unterschrift

Kurzfassung

Mit der hohen Durchdringung von dezentralen Energieressourcen (DERs) in Verteilernetzen ergeben sich viele Herausforderungen für den Netzbetrieb, insbesondere für die Spannungsregelung. Die auf einer Zustandsschätzung (SE) basierende Spannungsregelung für Verteilnetze nutzt Spannungsschätzungen, um zu berechnen, wie viel flexible Leistung erforderlich wäre, um die Spannungen innerhalb der gewünschten Grenzen zu halten. Die Wirksamkeit dieser Methode hängt von der Genauigkeit der SE ab, die verschiedenen Unsicherheitsquellen unterliegt. Die Installation zusätzlicher Zähler im Netz kann dazu beitragen, die Gesamtgenauigkeit zu erhöhen, aber die damit verbundenen Kosten für die Zähler müssen vor der Entscheidung über ihre Installation berücksichtigt werden.

Um wirtschaftliche Überlegungen bei der Verbesserung der SE zu berücksichtigen, wird in dieser Arbeit ein zweimoduliger Rahmen für die Durchführung einer Sensitivitäts- und Kosten-Nutzen-Analyse (KNA) der SE-basierten Spannungssteuerung entwickelt. Zunächst wird eine auf der Globalen Sensitivitätsanalyse (GSA) basierende Methodik für die Zählerplatzierung vorgeschlagen, die eine Top-Down-Prioritätenliste der zu installierenden Zähler erstellt, um die Genauigkeit der SE zu verbessern. Da die Installation zusätzlicher Zähler aus wirtschaftlicher Sicht sinnvoll sein sollte, werden die aus der Zählerplatzierung hervorgehenden Zähler einer Kosten-Nutzen-Analyse unterzogen, bei der die Kosten für die Installation eines zusätzlichen Zählers mit den Einsparungen an flexibler Leistung verglichen werden, die sich aus der Verbesserung der Spannungsregelungsstrategie mit dem installierten Zähler ergeben (im Sinne einer geringeren Leistungsflexibilität, die erforderlich ist, um die Spannung innerhalb der zulässigen Grenzen zu halten).

Der vorgeschlagene Rahmen wird angewandt, um verschiedene Szenarien mit unterschiedlichen Niveaus von Last, Erzeugung und DER-Durchdringung in einem repräsentativen 99-Knoten-Verteilungsnetz zu untersuchen. Die Ergebnisse zeigen den Einfluss der Betriebsbedingungen auf die Schätzungsunsicherheiten und unterstreichen die Bedeutung der Auswahl der besten Metrik für das DSO-Ziel, da die Zählerplatzierung die Ergebnisse der KNA stark beeinflusst. Es wird auch gezeigt, dass signifikante Einsparungen mit einer geringen Anzahl von Zählern erreicht werden können, insbesondere in Szenarien mit geringer Erzeugung, Last und DER-Durchdringung.

Das entwickelte Rahmenwerk weist aufgrund seiner Modularität genügend Flexibilität auf, z.B. kann die vorgeschlagene Zählerplatzierungsstrategie durch jede andere Zählerplatzierungsmethode ersetzt werden, ohne die KNA zu beeinträchtigen, spezifische Kosten können in das KNA-Modul aufgenommen werden, was die Replizierbarkeit des Rahmenwerks mit alternativen Randbedingungen sicherstellt, und die Zählerplatzierungsstrategie allein kann für jede andere SE-basierte Anwendung übernommen werden, falls wirtschaftliche Überlegungen nicht von Interesse sind. Darüber hinaus bietet der vorgeschlagene Rahmen den VNB ein neues Instrument, das ihnen hilft, fundierte Entscheidungen in Bezug auf betriebliche Aufgaben zu treffen: Durch die Verknüpfung der Zählerplatzierung mit der Spannungssteuerung und die Hervorhebung der wirtschaftlichen Vorteile können die VNB effektiv entscheiden, ob sich die Installation eines Zählers aufgrund von Kostenüberlegungen lohnt, anstatt nur Unsicherheitsschwellen zu berücksichtigen.

Stichwörter: Zustandsschätzung von Verteilernetzen, globale Sensitivitätsanalyse, Kosten-Nutzen-Analyse, zustandsschätzungsbasierte Spannungsregelung, Zählerplatzierung.

Abstract

With the high penetration of distributed energy resources (DERs) in distribution systems, many challenges arise in grid operation, particularly for voltage control. State-estimation (SE) based voltage control for distribution systems makes use of voltage estimates to calculate how much flexible power would be required to keep the voltages within desired limits. The effectiveness of this method depends on the accuracy of the SE, which is subject to different sources of uncertainty. The installation of additional meters in the grid can help to increase the overall accuracy, but the associated costs of the meters need to be considered before deciding on their installation.

To account for economic considerations in the process of improving SE, this thesis elaborates a two-module framework to perform a sensitivity and cost-benefit analysis (CBA) of the SE-based voltage control. First, a Global Sensitivity Analysis (GSA) based meter placement methodology is proposed, which produces a top-down priority list of meters to be installed to help improve the accuracy of the SE, and different ranking metrics are elaborated to reflect Distribution System Operators (DSOs)-specific objectives. Second, as the installation of additional meters should make sense from an economic point of view, the meters coming from the meter placement are subject to a CBA where the cost of installing an additional meter is compared with the savings in flexible power coming from the improvement of the voltage control strategy with the installed meter (in terms of lower power flexibility required to keep the voltage within the allowed boundaries).

The proposed framework is applied to study various scenarios with different levels of load, generation, and DER penetration, on a representative 99-node distribution grid. The results show the influence of operating conditions on the estimation uncertainties and highlight the importance of selecting the fittest metric for the DSO target, as the meter placement heavily influences the results of the CBA. It is also shown that significant savings can be achieved with a low number of meters, especially in scenarios with low generation, load, and DER penetration.

The developed framework showcases enough flexibility due to its modularity, e.g., the proposed meter placement strategy can be replaced by any other meter placement method without affecting the CBA, specific costs can be included in the CBA module ensuring the replicability of the framework with alternative boundary conditions, and the meter placement strategy alone can be adopted for any other SE-based application in the case economic considerations are not of interest. Moreover, the proposed framework provides DSOs with a new tool to help them in making informed decisions with respect to operational tasks: by linking the meter placement with the voltage control and emphasizing the economic benefits, DSOs can effectively decide if a meter is worth installing based on cost considerations rather than just accounting for uncertainty thresholds.

Keywords: Distribution Systems State Estimation, global sensitivity analysis, cost-benefit analysis, state estimation-based voltage control, meter placement.

Table of Contents

List of Figures

List of Tables

1 Introduction

Power distribution systems are currently experiencing significant changes due to the integration of distributed energy resources (DERs) such as solar photovoltaics (PV), wind turbines, electric vehicles (EVs), and energy storage systems (ESSs). The ever-increasing penetration of DERs, driven by a worldwide effort to reduce greenhouse gas emissions, and eventually reach carbon neutrality, comes along with increased volatility that can increase the number of voltage fluctuations, creating a negative impact on the quality and reliability of power supply. The previous makes voltage control a more critical issue in modern power distribution systems.

By making use of a State Estimation solution, the voltages in the grid can be estimated so that the DSOs are able to have a picture of the current operating conditions and consequently know if any voltages are outside of desired operational limits and act upon it to bring the voltages within desired limits. With the increasing penetration of DERs, one available strategy for DSOs to control the voltages is to make use of the new controllable resources available in the grids. SE-based voltage control, using the voltage estimates at the grid's nodes as a starting point, regulates the power setpoints of controllable sources in the grid to keep the voltages within acceptable limits. The voltage control is paired with an optimization algorithm to make sure that the minimum amount of power is being used to correct any possible voltage deviation, to minimize the associated costs. Since the voltage estimates come with an associated uncertainty, the voltage control must consider safety margins, in order to assure that the corrective actions actually keep the voltages within acceptable limits. The larger the uncertainties, the bigger the safety margins, and consequently, the bigger the necessary effort to correct voltage deviations, i.e., more power is required from the flexible sources to correct the deviations.

One way to reduce the safety margins, and the costs associated with the use of power flexibility, is to install meters in the grid to improve the accuracy of the state estimation. A good starting point of analysis is to devise a way of, a priori, identifying which type of meter, and in which grid location, can provide the largest uncertainty reduction to the state estimation results. In this context, a very helpful tool, and a not very used one in power systems applications, is Sensitivity Analysis, which has the purpose of answering this type of questions as part of its main characteristics. Loosely speaking, a meter that can reduce the uncertainty of the state estimation is eventually a meter that, if installed in the grid, is expected to reduce the costs of the associated required flexible power.

However, since the installation of the meters also carries a cost and considering the large sizes of distribution grids, and their traditional low levels of monitoring, this is not a straightforward task. Moreover, since the objective of meter installation, in this case, is to reduce the associated costs of flexible power used for voltage control, a cost-benefit analysis is needed to help in the decision of whether it makes sense or not to install a given meter since it allows to compare the cost of the meter versus the potential reduction in flexible power costs.

1.1 Literature Review

Although the use of sensitivity analysis is widespread in many scientific areas, its use in power system applications has been traditionally based on methods that perform a linearization of the problem or in the so-called “perturb and observe” methods, which is based on changing the value of a given quantity and observe its effect on another quantity. These methods, which fall under the category of “local” sensitivity analysis, are only able to perform a valid analysis around a specific operating point and, although they have been proven to be of help, they can only explore small changes in the inputs, thus becoming not so reliable for large disturbances, as the ones affecting today’s power systems because of the DERs penetration, especially for distribution grids [1].

The impact of uncertainties sources affecting state estimation and derived power systems applications has been studied before [2–4]. In [2], the effect of uncertainties sources on the state estimation-based voltage control of active distribution sources was studied, analyzing how the uncertainty of the estimated voltages affects the amount of power, and its associated cost, required for voltage control in active distribution grids. In [3] the effect that various inputs, like measurement uncertainties, measurement configuration, and load levels, have on the estimated voltage magnitudes is analyzed. In [4] the impact that the sources of uncertainty in the modeling of distribution lines have on power flow calculations is studied by looking at the variability of the voltage profile. However, in these, only uncertainty analysis is performed, i.e., the uncertainty of the affected quantities was quantified, but it wasn’t apportioned to the uncertainty sources originating it.

The use of sensitivity analysis for state estimation studies has been previously reported in the literature [5, 6], however, these only make use of “local” sensitivity analysis techniques. The use of more effective Sensitivity Analysis methods, falling in the category of “global” sensitivity analysis, is then necessary to study a range of operation wider than the baseline conditions. Although these “global” methods have also been used for power systems applications in the literature, as in [7, 8] or in [9] where a preliminary optimal meter placement strategy based on global sensitivity analysis is sketched out, they still have not been used much on State Estimation or State Estimation-based applications.

Although the use of optimal meter placement strategies in the literature has been extensively reported [10–14], existing references usually have as goal the reduction of the estimation uncertainties below a given threshold using a minimum number of meters or to minimize the estimation uncertainties using a fixed number of meters. These optimization objectives are selected without any connection to grid management tasks that rely on state estimation results, which does not allow for an evaluation of the benefits that the installation of a specific meter on the grid could have on said management tasks. An approach that would allow performing this evaluation is an important planning tool that helps DSOs to justify or discard the installation of new meters based on, for example, the economic viability of installing a new meter by comparing the cost of the meter versus savings obtained by the improvement of an operational task due to the installation of the meter, as done in this thesis.

1.2 Thesis objectives

The objective of this thesis is to propose a meter placement strategy based on global sensitivity analysis (GSA) and to propose a cost-benefit analysis framework that uses the meter placement results to evaluate the economic viability of installing the suggested meters, comparing the costs of installing the meter with savings obtained in operational costs associated to voltage control. Specifically, the thesis focuses on the following research questions:

- How can Global Sensitivity Analysis be used to derive a meter placement strategy, which inputs should be considered, and how should the meter placement problem be posed?
- What are the cost benefits of improving SE by installing new meters compared to keep using flexible power, considering factors such as investment costs, operational costs, and DER and ESS penetration?

The contributions of this thesis are twofold. First, a systematic methodology for meter placement based on SA of the SE is provided, which can help distribution system operators (DSOs) to enhance the results of their SE algorithms and improve the reliability and efficiency of their networks. Second, a methodology for performing a cost-benefit analysis of state estimation-based voltage control is developed, which can help decision-makers to assess the economic feasibility of installing new meters and make informed investment decisions.

The rest of this thesis is organized as follows:

- Chapter 2 “Theoretical background” describes the theoretical background for this thesis, including global sensitivity analysis, Polynomial chaos expansion, state-estimation, and voltage control algorithm.
- Chapter 3 “Framework” describes the proposed meter placement strategy based on sensitivity analysis and the proposed cost-benefit analysis methodology to decide on the installation of new meters, as well as how these two parts are tied together. It is also included a description of the distribution system models used and specifics on the implementation of uncertainty and sensitivity analysis, and the voltage control algorithm.
- Chapter 4 “Results and Discussion” presents the results and discussion of the simulations done, pertaining to the meter placement strategy and cost-benefit analysis.
- Chapter 5 “Conclusions and Future Work” provides the conclusions and future work of the thesis.

2 Theoretical background

This chapter deals with the presentation and explanation of all the mathematical tools used for this thesis. The aim is to present Sensitivity Analysis (SA), a metamodeling tool, the Polynomial Chaos Expansion (PCE) metamodeling tool, State Estimation (SE), and a Voltage Control algorithm.

Section 2.1 deals with presenting Sensitivity Analysis, its difference with respect to Uncertainty Analysis (UA), and the variance-based Method used in this thesis. Section 2.2 presents the Polynomial Chaos Expansion, a metamodeling tool that aids in performing the SA by means of a surrogate model. Section 2.3 presents the State Estimator implementation used for this work, briefly introducing state estimation in power systems and the specific formulation used. Lastly, section 2.4 presents the Voltage Control Algorithm, which is a key part of the Cost-Benefit analysis.

2.1 Sensitivity Analysis

Sensitivity Analysis is a powerful technique that, generally speaking, studies how the variability in the inputs of a model affects the variability of the model's output, where the model could be any numerical procedure or algorithm that replicates the behavior of a real-life phenomenon, and the inputs can be the type and structure of the model, model equation parameters, initial and boundary conditions, resolution levels, etc. These inputs are subject to sources of uncertainty like data imprecision, own randomness of the model, etc. [1]. More specifically, SA attempts to attribute the variability of the model output to each of the inputs. This makes SA an important tool in decision-making processes because it helps to provide valuable insights into the results obtained from complex models or simulations and how these results are affected by the inputs, which in turn gives hints as to what the effectiveness of a corrective action (any action taken to reduce the uncertainty of an input, or inputs) might be.

As a general guide, performing SA helps to answer questions like [1]:

- Which inputs produce the largest variation in the model output?
- Which inputs do not influence the model output?
- How much is the variability of the model output reduced by reducing the uncertainty of a given input?

2.1.1 Uncertainty Analysis

A very closely related concept to SA is Uncertainty Analysis (UA). while SA can be defined as the study of how the uncertainty of the model output can be attributed to each of the model inputs, UA can be defined as the characterization of the model output uncertainty, affected by the inputs' uncertainty [1]. The method used for performing UA is chosen depending on the nature of the uncertainty of the inputs [9]. If the inputs are random variables defined by a Probability Density Function (PDF), combinations of the inputs within their respective PDF can be used to evaluate the model and produce a set of output values from which an empirical distribution histogram can be computed. The most used

method for the previous cases is the Monte Carlo Simulation (MCS) [15]. A brief description of MCS is given next.

Given a general model $y = f(\boldsymbol{x})$ relating the inputs to the outputs, where $\boldsymbol{x} = [x_1, x_2, \dots, x_n]$ is the vector of the inputs and y is the model output, and the uncertainty of each input is defined by a corresponding PDF. Each of the model inputs is sampled within its respective PDF to obtain N different combinations of inputs, for which the model is evaluated, obtaining N corresponding values of y that represent the output distribution and from which the expectation and the variance can be estimated.

The simplicity of the method is what makes it so widely used, however, to assure that the N values of y are representative of the true output distribution, a large number of input combinations has to be used. This makes MCS suffer from scalability problems that might make it not feasible, or too time-consuming, to use it.

When performing SA, the use of UA becomes necessary, as characterizing the output uncertainty is needed to then attribute its variability to the variability of the inputs. Figure 1 shows a general depiction of how UA and SA are related.

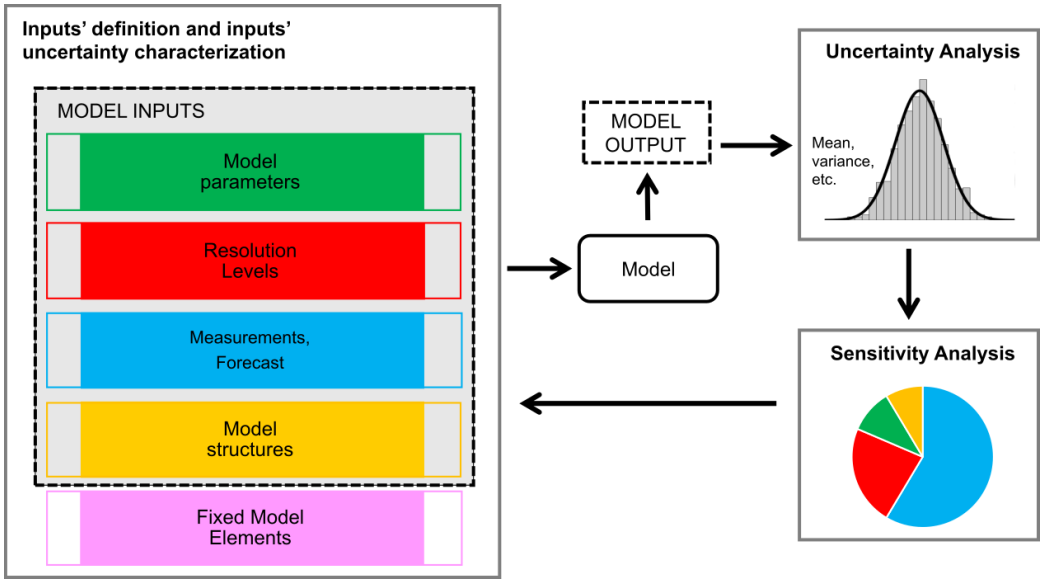

Figure 1. General depiction of the connection between SA and UA [1].

2.1.2 Sensitivity Analysis classification

The SA methods can be classified based on their exploration of the input space, in "local" or "global" methods, and based on their sampling strategy, in "One-At-a-Time" (OAT) or "All-At-a-Time" (AAT). Local methods only explore small, or local, changes of the inputs around a given baseline, i.e., only a portion of the input PDF is considered. Global methods, on the other hand, aim to explore (at least conceptually) the entirety of the inputs PDFs. OAT methods, as the name indicates, only consider the variation of one of the inputs at a time, while maintaining the other inputs fixed at a given value. On the opposite, AAT methods consider the variation of all the inputs at the same time, for example, as done in MCS. Although the One-at-a-time methods intuitively help to explain how much the variability

of the considered input affects the variability of the model output, they do not account for the possible interactions between the inputs [1].

For the work of this thesis only a "global", AAT method was used, the chosen method is explained in the next subsection.

2.1.3 Variance-based Sensitivity Analysis

Variance-based SA comprises a group of global AAT SA methods that are based on the decomposition of the model output variance into contributions from the individual inputs and contributions from the possible input interactions. The method used in this thesis is the so-called Sobol' or Sobol' indices method [16]. A description of the method is presented next taken from [1], a more detailed explanation can be found in [16, 17].

Considering again the generic model used in Section 2.1.1, the main idea in variance-based methods is to consider the question of how much the variability of the model output, $Var(y)$, changes when we fix a given model input, x_i, to its "true" value x_i^*. It is expected that the conditional variance of the output, $Var(y|x_i = x_i^*)$, is lower than the original variance, $Var(y)$, since one of the sources of uncertainty has been eliminated. Since x_i^* cannot be known, a reasonable choice is to evaluate the conditional variance over all the possible values of x_i and compute the expected value of the conditional variance, while all other variables are varied in their respective PDFs, i.e., $\mathbb{E}_{x_i}(Var_{x_{\sim i}}(y|x_i = x_i^*))$. Given the law of total variance:

$$Var(y) = \mathbb{E}_{x_i}\left(Var_{x_{\sim i}}(y|x_i)\right) + Var_{x_i}\left(\mathbb{E}_{x_{\sim i}}(y|x_i)\right) \tag{1}$$

where $\mathbb{E}_{x_i}\left(Var_{x_{\sim i}}(y|x_i)\right)$ is the residual output variance, and $Var_{x_i}\left(\mathbb{E}_{x_{\sim i}}(y|x_i)\right)$ can be interpreted as the reduction in the model output variance, obtained by fixing x_i to its "true" value x_i^*, i.e. if the uncertainty of input x_i were to be eliminated. From the previous definitions, it is expected that a very influential input variable x_i would have a larger variance reduction value than other not-so-influential input variables. Therefore, this value can be used as a measure of how influential an input is for the model output, in other words, as a measure of the sensitivity of y to x_i. With the previous in mind, the first-order Sobol' Index for variable x_i can be computed with:

$$S_i = \frac{Var_{x_i}\left(\mathbb{E}_{x_{\sim i}}(y|x_i)\right)}{Var(y)} \qquad with\ S_i \in [0,1] \tag{2}$$

As defined before, S_i is a measure of how important an input x_i is to the variability of the model output, or in other words, how much of the variability of the model output, y, can be attributed solely to the variability of input x_i. This also allows to perform a ranking of the inputs, from more influential to least, by sorting the computed sensitivity indices (SIs). However, while a high value of S_i indicates that the input x_i is important, a low value of S_i, cannot be interpreted as x_i being not important. The definition of the first-order index omits the combined effect that the selected input might have on the

model output by interacting with the other variables since the conditional variable is computed by fixing just one of the variables.

As a solution to this problem, higher-order Sobol' Indices can be defined, similarly to Equation (2). For example, the Second-order Index, S_{ij}, is a measure of the combined contribution that inputs x_i and x_j have in variability of the model output. The higher-order indices can be computed up until the M_{th} order, with M being the number of inputs of the model. Although the higher-order indices provide a very detailed decomposition of the model output variance, the computation of all the higher-order indices can easily become an unfeasible task, since there will be as many as $2^M - 1$ terms in the decomposition. For a model with only 10 inputs, this means that 1023 terms would have to be computed.

As a workaround for the dimensionality problem, the total-order Sobol' Indices are introduced as:

$$T_i = \frac{\mathbb{E}_{x_{\sim i}}\left(Var_{x_i}(y|x_{\sim i})\right)}{Var(y)} = 1 - \frac{Var_{x_{\sim i}}\left(\mathbb{E}_{x_i}(y|x_{\sim i})\right)}{Var(y)} \tag{3}$$

where $Var_{x_{\sim i}}\left(\mathbb{E}_{x_i}(y|x_{\sim i})\right)$ is the variance reduction that is obtained, on average, if the uncertainties of all the inputs, except x_i, could be eliminated, and $\mathbb{E}_{x_{\sim i}}\left(Var_{x_i}(y|x_{\sim i})\right)$ is the residual model output variance. T_i can then be interpreted as the overall contribution of variable x_i to the output variance, including all higher-order interactions of x_i. For example, for a model consisting of three variables, $T_1 = S_1 + S_{1,2} + S_{1,3} + S_{1,2,3}$. If the total-order index for a variable x_i is close to zero, this variable can be considered as not important, since neither the self-influence nor the interactions of x_i with all the other variables have an impact on the model output variability.

For variance-based sensitivity indices, the following properties hold true:

- $0 \leq S_i \leq T_i \leq 1$ if the inputs are independent
- $\Sigma_i^n S_i \leq 1$ if the inputs are independent
- $\Sigma_i^k S_i = 1$ if there are no input interactions in the model
- $T_i - S_i$ measures how much x_i is involved in interactions with other inputs
- $1 - \Sigma_i^n S_i$ indicates the overall interactions among inputs

As an example, let us consider the following toy model:

$$y = f(x) = x_1^2 - x_2 + 4x_1x_3 \tag{4}$$

Where y is the model output and $x = [x_1, x_2, x_3]$ is the vector of random input variables, assumed to be independent for this example. x_1 has a Uniform PDF in the range [-0.5,0.5], x_2 has a Uniform PDF in the range [0.5,1.5], and x_3 has a Uniform PDF in the range [0,1]. The values of the sensitivity indices are shown in Table 1.

Table 1. Sensitivity Indices for example model.

First Order S_i	Total Order T_i	Second Order S_{ij}	Third Order S_{ijk}
$S_1 = 0.64$	$T_1 = 0.84$	$S_{12} = 0.00$	$S_{123} = 0.00$
$S_2 = 0.16$	$T_2 = 0.16$	$S_{13} = 0.20$	
$S_3 = 0.00$	$T_3 = 0.20$	$S_{23} = 0.00$	

From the sensitivity indices, it can be seen that the input that would bring a bigger reduction in the output variability, if its uncertainty were to be eliminated, is x_1, which is expected since the model is a sum of three terms of which two depend on x_1, and one of those is squared. This means that if some corrective action could be made on one of the inputs to reduce its uncertainty, with the intention of reducing the model output variability, it would make the most sense to do it on x_1, assuming that it takes the same effort, in terms of money, time, etc., to reduce the uncertainty of any input.

Another thing to notice is that even though S_3 is null, variable x_3 cannot be regarded as non-important, as explained before, and T_3 confirms that it does have some influence on the model output, as can be expected just by looking at the model. In this case all the influence of x_3 is of second order, i.e., it has a combined effect with one of the other inputs, x_1 in this case.

When computing the variance-based sensitivity indices with methods like the one in [18] the computational cost for obtaining the full set of first and total order indices is $N(M+2)$ model runs, where N is the sample size, usually between a few hundreds to a thousand. This becomes very computationally expensive for a high number of input variables or if each of the model evaluations takes time in the order of seconds to minutes. For this, several methods have been proposed in the literature, among them the use of metamodels as in [17].

2.2 Polynomial Chaos Expansion

As mentioned before, the computation of the Sobol' Indices might become computationally too expensive, one way of overcoming this limitation is the use of metamodeling tools, the chosen method for this thesis was the use of Polynomial Chaos Expansion as proposed in [17]. This method builds a surrogate model to represent the input-output relation of the original model, from this surrogate model the sensitivity indices can be more easily computed. A brief explanation of the method is given next based on [9, 17, 19], for a more detailed explanation the references should be revised.

Consider a vector $X \in \mathbb{R}^M$ of independent random variables, each with its own PDF, and a generic model $y = f(X)$. The PCE of $f(X)$ is defined as:

$$y = f(X) = \sum_{\alpha \in \mathbb{N}^M} y_\alpha \Psi_\alpha(X) \tag{5}$$

where the $\Psi_\alpha(X)$ are multivariate polynomials orthonormal with respect to the PDFs of the elements of X, $\alpha \in \mathbb{N}^M$ are the indices that identify the components of the multivariate polynomials and the $y_\alpha \in \mathbb{R}$ are the corresponding coefficients.

Although the sum in Equation (5) has infinite terms, it must be truncated in practical applications to create the truncated PCE defined as:

$$f(X) \approx f^{PC}(X) = \sum_{\alpha \in \mathcal{A}} y_\alpha \Psi_\alpha(X) \tag{6}$$

where $\mathcal{A} \subset \mathbb{N}^M$ is the set of selected indices of the multivariate polynomials, which is done by defining a total-degree truncation scheme, where all polynomials of degree lower or equal to p are selected. The total number of terms in the series K grows exponentially with the degree p and is given by:

$$K = \frac{(M+p)!}{M!\,p!} \tag{7}$$

In many applications not all terms are equally important. Often, the important terms tend to be the ones where only a few variables are involved, according to the sparsity of effects principle. One modification to the original scheme is the hyperbolic, or q-norm, truncation scheme, which makes use of the q-norm ($q \in (0,1]$) to define the truncation [20]:

$$\mathcal{A}^{M,p,q} = \{\alpha \in \mathcal{A}^{M,p} : \|\alpha\|_q \leq p\} \tag{8}$$

where:

$$\|\alpha\|_q = \left(\sum_{i=1}^{M} \alpha_i^q\right)^{1/q} \tag{9}$$

Figure 2 shows an example of how the truncation behaves in two dimensions for different values of p and q. For $q = 1$, first row of the figure, the hyperbolic scheme is the same as the total-degree scheme, for example, for $p = 3$, the total number of terms is 10. By reducing the value of q, columns in the figure, the total number of terms is reduced, for example, for $p = 3$ and $q = 0.5$, the total number of terms is reduced to 7.

Once the PCE coefficients have been obtained, the evaluation of the metamodel on new samples becomes a matter of using Equation (6), this is a very efficient operation that comes at a computational cost of only evaluating the polynomials and a small number of matrix multiplications, which can be used to obtain the PDF of the model output. Another important property of the PCE is that the coefficients can be used to efficiently compute the Sobol' Indices, for a more detailed explanation see [21].

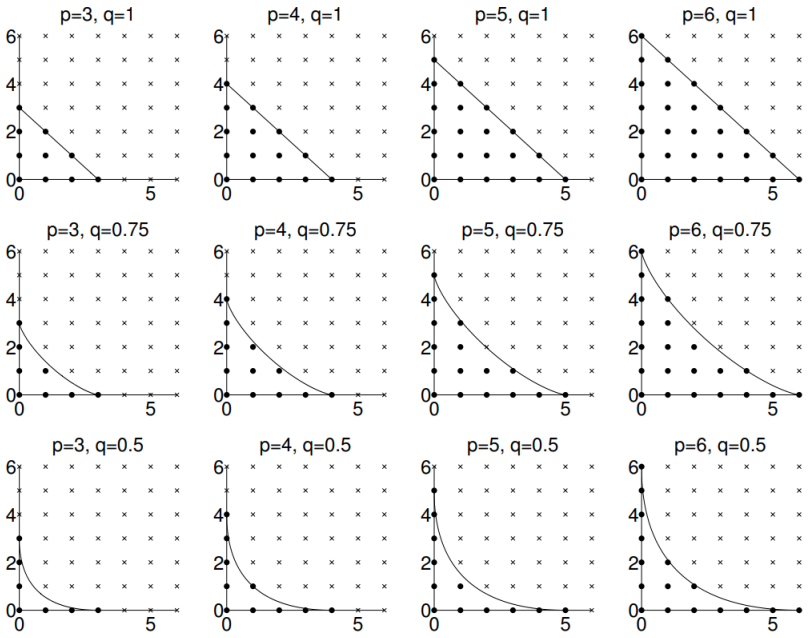

Figure 2. Hyperbolic truncation for various p and q values [19].

2.3 State Estimation

State Estimation (SE) is the process by which the states of a system (i.e., the set of variables that completely describe the current state of a system), are estimated based on the knowledge of the behavior of the system under study, the system model, and a set of measurements about its operating conditions. In the context of power systems, the states of the system are usually the set of complex node voltages, from which any other grid variable, for example, branch currents or power flows, can be calculated. For this, a set of measurements coming from different monitoring devices, including voltmeters, power injection meters, power flow meters, PMUs, etc. is used together with information on the topology of the grid, status of switches, and equations modeling the different elements of the system and the relations between system variables, like power flow equations.

The process of state estimation is vital for ensuring that power systems are operated in a reliable and secure manner. The accurate representation of the system's current state allows operators to make informed decisions and take appropriate real-time control actions. The information provided by state estimation is crucial to obtain system awareness, estimate the conditions of the system during contingencies, and monitor system stability. Additionally, this information is the base for many other advanced applications such as optimal power flow, contingency analysis, and system planning. Figure 3 shows a general picture of the state estimation framework in power systems.

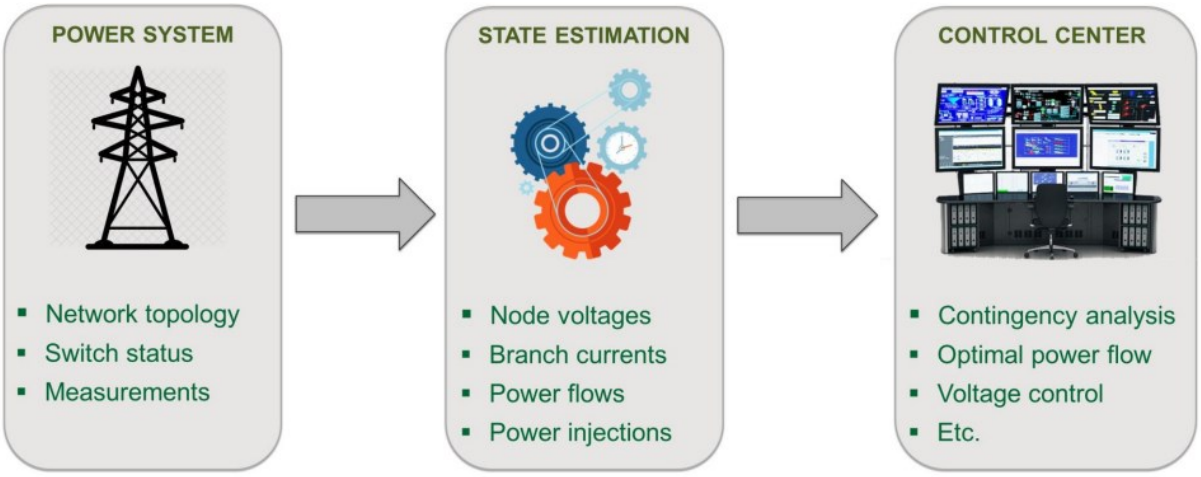

Figure 3. State Estimation framework in power systems. [22]

2.3.1 State Estimation implementation

The implementation of state estimation for power systems is not unique and depends on several factors. One of these factors can be the selection of the states, for example, different groups of grid-related quantities can be selected as the states to be estimated, one of the more straightforward selections would be to use magnitudes and angles of the grid voltages, however, another valid selection could be the one composed of the complex voltage at a given reference node in the grid and the set of complex currents for all the branches of the grid. In principle, any set of variables, that once known allow for the computation of any other grid quantity, is a valid selection for the states of the system.

Another factor that influences the implementation of the state estimation is whether the grid under study is a distribution or a transmission grid, for example, in transmission grids some simplifications can be made to the system equations due to the high X/R ratio, small angle differences and low variability of voltage magnitudes. These simplifications do not hold true for distribution systems. Also, while transmission grids are highly monitored grids with many voltage and power measurements available, on the other hand, distribution grids have a low level of monitoring, with usually very few voltage measurements available, which brings a challenge on how to achieve accurate results with fewer available measurements.

For the estimation of the states, there are different mathematical models available, Weighted Least Squares (WLS), Maximum Likelihood Estimation (MLE), and Kalman Filter (KF), among others. The most widely use of these is the WLS which is the method used in this thesis and will be presented next.

2.3.2 State Estimation formulation

The specific State Estimation implementation used for this thesis is the one presented in [2], the explanation of the formulation, the choice of the state vector, and the general estimation algorithm are explained next.

The general formulation of a state estimator for power systems is usually based on:

$$z = h(x) + e \tag{10}$$

where $x = [x_1, x_2, \dots, x_N]^\intercal$ is the vector of the state variables, $h(x) = [h_1(x), h_2(x), \dots, h_M(x)]^\intercal$ is the vector of the measurement functions, which links the state variables to the measurements in the measurement vector $z = [z_1, z_2, \dots, z_M]^\intercal$, and e is the vector of measurement errors corresponding to z. The measurement vector includes all the available measures, the ones coming from measuring devices installed in the grid, and the so-called pseudo-measurements, information known a priori about the power at the nodes, usually from historical or statistical data.

The state vector used in this implementation is:

$$x = \left[V_{ref}^r, V_{ref}^x, I_1^r, I_1^x, \dots, I_{N_{br}}^r, I_{N_{br}}^x\right]^\intercal \tag{11}$$

where V_{ref}^r and V_{ref}^x are the real and imaginary parts, respectively, of the complex voltage at a previously chosen reference node in the grid, I_i^r and I_i^x are the real and imaginary parts of the complex current flowing through the i-th branch of the grid. In the case that no PMUs are available in the grid, V_{ref}^x is removed from the state vector since angles have to be defined relative to the angle of the voltage at the reference node, which is set to zero.

To estimate the states a WLS approach is used to solve the minimization:

$$\hat{x} = \min_x [z - h(x)]^\intercal W [z - h(x)] \tag{12}$$

Where W is a weighting matrix defined as the inverse of the covariance matrix of the measurements, that gives more importance to the more accurate measurements. The covariance matrix is obtained as:

$$Cov = \begin{bmatrix} \sigma_1^2 & 0 & \cdots & 0 \\ 0 & \sigma_2^2 & \dots & 0 \\ \vdots & \vdots & \ddots & \vdots \\ 0 & 0 & \cdots & \sigma_M^2 \end{bmatrix} \tag{13}$$

Where σ_i is the standard deviation associated with the i-th measurement.

The minimization problem in (12) is solved with an iterative process consisting of three steps for each iteration. The first step is preparing the measurements, for this, phasor measurements are expressed in rectangular coordinates, and power measurements are transformed into equivalent current measurements according to:

$$I_{eq}^{r} + I_{eq}^{x} = \frac{P - jQ}{v^{*}} \tag{14}$$

where $S = P + jQ$ is the complex power considered as measurement and v^{*} is the complex conjugate of the estimated voltage phasor at the previous iteration for the considered node.

The second step is to obtain the updated (for the current iteration) state estimates by solving the normal equations according to:

$$\hat{x}_k = \hat{x}_{k-1} + (H^{\intercal}WH)^{-1}H^{\intercal}W[z_k - h(x_{k-1})] \tag{15}$$

Where H is the Jacobian of the measurement functions and k is the current iteration.

The third and final step is the update of the voltage estimates making use of the current state vector estimate, computed with (15), and a forward sweep according to:

$$v = \hat{v}_{ref,k}1 - Z_{nod}\hat{\imath}_k \tag{16}$$

Where 1 is a column vector of ones, $\hat{\imath}_k$ is a vector containing the branch currents estimates at the current iteration and Z_{nod} is a matrix whose i-th row contains the impedances of the branches in the path from the reference node to the node i. These three steps are then iteratively repeated until the difference in the state estimates between the previous iteration and the current one fall below 10^{-6} for all the state variables.

After the iterative process is terminated, the uncertainties of the voltage and currents estimates can be computed by computing the inverse of the gain matrix G defined as:

$$G = H^{\intercal}WH \tag{17}$$

Where the elements of the inverse of the G matrix represent the variance of the estimates. The uncertainty of the estimates in percentage is then computed, assuming a Gaussian distribution and a coverage factor of 3, as:

$$U_{est,i} = 300 * \frac{\sigma_i}{x_i}\ \% \tag{18}$$

Where σ_i is the standard deviation of the i-th estimate and x_i is the estimated value of the i-th state. Since the states are selected as the real and imaginary parts of voltages and currents, the values extracted from the inverse of the gain matrix have to be transformed if the uncertainty of a magnitude estimate is to be computed.

2.4 Voltage Control Algorithm

The main objective of the voltage control algorithm is to keep the voltage magnitudes in the grid within desirable limits by regulating the reactive and active power setpoints of available flexible sources in the grid, like Energy Storage Systems, PV modules, Wind Turbines, Distributed Generation, etc. The voltage control algorithm used for this thesis is the one presented in [2] and is explained next.

The voltage control algorithm is based on a centralized constrained optimization to keep the grid's voltages within the predefined limits, it builds from a linearized branch flow model that approximates the relation between node voltage magnitudes and the injected active and reactive power at the nodes according to:

$$V = 1V_0 + RP_{inj} + XQ_{inj} \tag{19}$$

where V_0 is the voltage magnitude at the main substation, V is a vector containing all the bus voltage magnitudes, P_{inj} and Q_{inj} are vectors containing the active and reactive power injections at each node, and R and X are the real and imaginary parts of the impedance matrix Z, which is obtained from:

$$\begin{bmatrix} Z & 1 \\ 1^{\intercal} & 0 \end{bmatrix} = \begin{bmatrix} Y & 1_0 \\ 1_0^{\intercal} & 0 \end{bmatrix}^{-1} \tag{20}$$

Where Y is the admittance matrix of the grid and 1_0 is a column vector with the first element equal to 1 and the rest equal to 0.

From (19), it can be derived a way of modifying the voltage magnitude profile of the grid by adjusting the active and reactive power injections of flexible sources following:

$$V_c = 1V_0 + RP_{inj} + XQ_{inj} + R\Delta P + X\Delta Q \tag{21}$$

Where V_c is the resulting voltage magnitudes after the adjustment of the power injections, and ΔP and ΔQ are the changes in power setpoints requested to the flexible sources.

The goal of the used optimization algorithm is to minimize the overall power variations requested to the flexible sources (FS) to keep the voltage magnitudes between the predefined limits. With this in mind, the effect of the power variations on the voltage profile is considered by weighting active power changes with R and reactive power changes with X. The objective function of the optimization is then defined as:

$$J(\Delta P_{FS}, \Delta Q_{FS}) = \Delta P_{FS} R \Delta P_{FS} + \Delta Q_{FS} \mathrm{X} \Delta Q_{FS} \tag{22}$$

The constraints used for the optimization problem are based on the operational limits of the available flexible sources, i.e., the maximum and minimum power setpoints and the boundaries for the grid voltages. The first constraint depends on the type of available flexible sources, if we consider ESSs and DGs are available, it could be expressed as:

$$-P_{ch,i}^{max} \leq \Delta P_{ESS,i} \leq P_{dis,i}^{max} \quad \forall i = 1, \dots, N \tag{23}$$

$$-Q_{DG,i}^{max}(t) \leq \Delta Q_{DG,i} \leq Q_{DG,i}^{max}(t) \quad \forall i = 1, \dots, N \tag{24}$$

$$-P_{DG,i}^{max}(t) \leq \Delta P_{DG,i} \leq 0 \quad \forall i = 1, \dots, N \tag{25}$$

Where $P_{ch,i}^{max}$ and $P_{dis,i}^{max}$ are the maximum charging and discharging power for the Storage System located at the i-th node, $Q_{DG,i}^{max}$ is the maximum reactive power for the i-th Distributed Generator, and $P_{DG,i}^{max}$ is the generated active power for the i-th Distributed Generator at the considered time t. The limits would be set to zero in all the nodes where no ESS or DG are available.

The second constraint can be expressed as:

$$\Delta V(t) \leq V^{max} - \hat{V}(t) + \Delta V(t-1) \tag{26}$$

$$\Delta V(t) \geq V^{min} - \hat{V}(t) + \Delta V(t-1) \tag{27}$$

Where V^{max} and V^{min} are vectors containing the upper and lower boundary for each of the voltage magnitudes, $\hat{V}(t)$ is the vector of the estimated voltage magnitudes at the time t, coming form the State Estimation, and ΔV is the resulting voltage variation due to the power setpoints adjustments. The resulting voltage variation form the previous step, $\Delta V(t-1)$, is included in the second constraint to make sure that the power adjustments are kept over time as long as they are needed, without relaxing the adjustments when the State Estimation sees a better voltage magnitude coming for the very same power adjustment.

Since the estimated voltage magnitudes have an associated uncertainty, calculated as in section 2.3.2, equations (26) and (27) are modified to restrict the constraint and ensure that corrected voltage magnitudes will remain within limits regardless of the deviation between the actual voltage and the estimated value. For example, the desired unmodified voltage bounds used for this thesis are 0.95 and 1.05 p.u., if one of the voltage magnitudes has an estimation uncertainty of 2.5% then the bounds are modified to 0.975 and 1.025 p.u. by following (28) and (29).

$$V^{min} = 0.95 + \frac{U_{est}}{100} \tag{28}$$

$$V^{max} = 1.05 - \frac{U_{est}}{100} \tag{29}$$

where V^{max} and V^{min} are the same as in equations (26) and (27), and U_{est} is a vector containing the estimation uncertainties of the voltage magnitudes. This ensures that the voltage always stays within the desired boundaries regardless of the negative impact of the state estimation uncertainties.

In summary, the optimization problem is a quadratic optimization with linear inequality constraints and can be formulated as:

$$\min_{\Delta P_{FS}, \Delta Q_{FS}} J(\Delta P_{FS}, \Delta Q_{FS}) \tag{30}$$

Subject to (23), (24), (25), (26), (27), (28), (29)

3 Framework

This chapter focuses on the framework developed in this thesis and the specifics of the implementation of the concepts explained in the Theoretical background chapter. Section 3.1 deals with the two grids used for the simulations, a toy grid used for preliminary analyses, and a real distribution grid. Section 3.2 explains how the state estimation is performed and what states and inputs are considered. Section 3.3 deals with the uncertainty and sensitivity analysis of the state estimator and explains what inputs, with their respective uncertainties, and outputs are considered. Section 3.4 explains the proposed meter placement methodology based on the results of the GSA. Lastly, section 3.5 explains the cost-benefit analysis (CBA) methodology conceived to define the best metering infrastructure considering the meter placement results and the requirements of the voltage control algorithm.

The implementation of the framework is done by making use of MATLAB and is divided into two main modules, the first is a meter placement algorithm based on GSA which takes as inputs the current meter configuration of the grid under study and the set of possible meters to install and produces a top-down ranked list of meters that successively bring the highest reduction to the uncertainty profile of the magnitude estimates. This list of meters is then used as input to the second part, a Cost-Benefit analysis, that evaluates the economic viability of the installation of each meter to make the final decision of which of the meters to install.

Figure 4 shows the general layout of the framework. It is worth noting that the implementation was made to allow the replacement of any of the parts for similar, or potentially different, analysis.

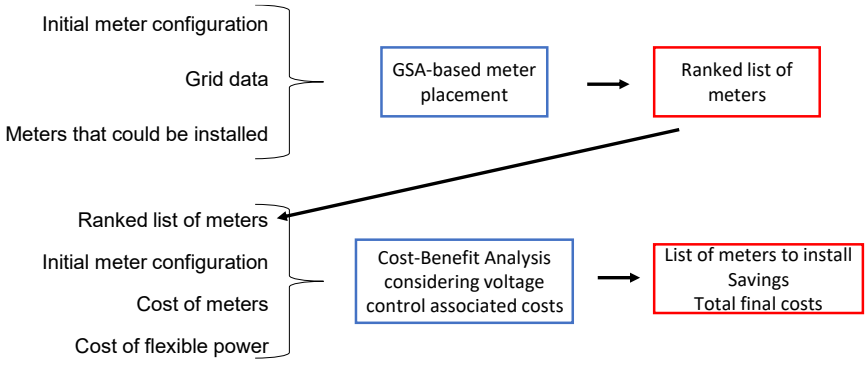

Figure 4. High-level representation of the two-module developed framework.

3.1 Distribution System Model

During the work of this thesis two different grids were used, a small 10-node toy grid, used to develop the meter placement methodology, to do initial tests of all the different codes that were implemented, and used in this chapter to better explain the different methodologies; and an industrial 99-node representative MV distribution grid used to provide a realistic scenario for testing the scalability and performance of the meter placement and running the cost-benefit analysis simulations, taking advantage of the available yearly profiles.

3.1.1 Toy grid

The 10-node toy grid is a sample grid created mainly with the idea of testing and developing the meter placement methodology. The grid consists of two feeders, each with one generator, and loads at every other node, except for the slack bus. Since no time series profiles exist for this grid the cost-benefit analysis cannot be tested on this grid, only the meter placement procedure is applied to the grid. The one-line diagram of the grid can be seen in Figure 5.

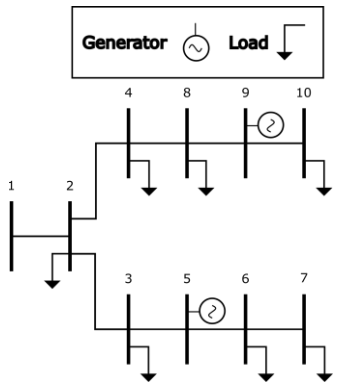

Figure 5. One-line diagram of the toy grid.

3.1.2 Industrial Distribution grid

A 99-node MV distribution grid was also used to test the meter placement procedure and the cost-benefit analysis. This grid is an industrial distribution grid from the Atlantide research project [23–25]. The network consists of 99 nodes and 7 feeders with several distributed generators, including 3 Wind generators, 22 PV plants, and 3 CHP plants; and a mix of industrial, commercial, and residential loads. Yearly, monthly, weekly, and daily profiles are available for the grid. These profiles allow us to account for different loading and generation operating conditions and are an important part of the cost-benefit analysis. The one-line diagram of the grid can be seen in Figure 6.

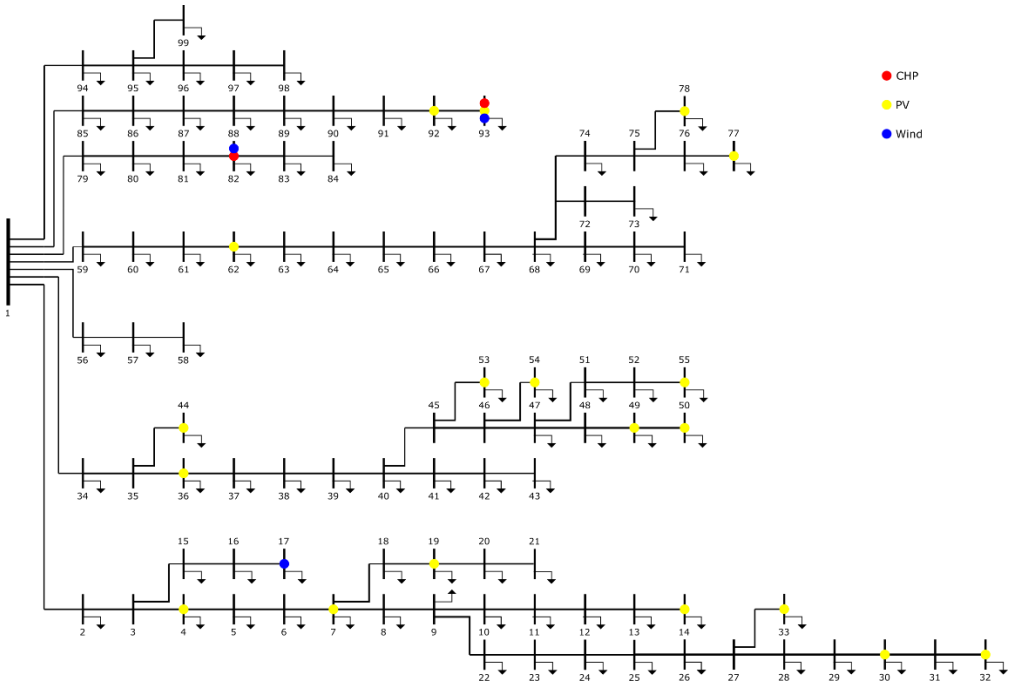

Figure 6. One-line diagram of the 99-node grid.

Irrespective of the grid that is used, some data needs to be read and prepared for the subsequent calculations, this includes topological information of the grid, line parameters, and current set points for loads and generation.

3.2 State-Estimation

The state estimator explained in Section 2 is used for two main purposes:

- to obtain a set of estimated voltage magnitudes given a certain operating condition and meter configuration, and from those values perform uncertainty and sensitivity analysis of the state estimator for the meter placement procedure;
- as a means to estimate the uncertainty of the voltage estimates which are inputs to the voltage control algorithm.

Before estimating the states, a power flow is run on the grid using current operating conditions to obtain the real values of the voltage magnitudes and power flows. Additionally, a given meter configuration, including pseudo-measurements, and respective uncertainties are provided. The uncertainties given for power injection and power flow meters are assumed to be the uncertainty for both active and reactive power measurements. The creation of the measured data is done by sampling N times a normal distribution using as the mean the real voltage magnitude, power flow, or power injection value, depending on the type of meter or pseudo-measurement, and as standard deviation the value calculated with:

$$\sigma = U * \frac{V}{3 * 100\%} \tag{31}$$

Where U is the measurement uncertainty in %, V is the real value obtained from the power flow and the factor of three is to account for the coverage factor. For each of the N sets of measured data, a respective set of estimated voltage magnitudes is obtained. The value of N depends on the purpose of the estimation, for the uncertainty and sensitivity analysis performed in this thesis, a value of at least 1000 was used, and for the voltage control 1 was used.

3.3 Uncertainty and Sensitivity Analysis

To perform the uncertainty and the sensitivity analysis the outputs from the power flow and state estimator are required. For the uncertainty analysis the set of N estimated voltage magnitudes for each node of the grid and the true values of the voltage magnitudes are used to compute the extended uncertainty in % of the voltage magnitude estimates according to (32), similar to [12].

$$U_{\hat{V}_i} = \sigma_{\hat{V}_i - V_i} * \frac{3 * 100\%}{V_i} \tag{32}$$

Where $U_{\hat{V}_i}$ is the extended uncertainty in percentage for node i, $\sigma_{\hat{V}_i - V_i}$ is the sample standard deviation of the difference between the magnitude estimates and the true value for node i, and 3 is the coverage factor. From the calculated uncertainties of the estimated magnitude, an uncertainty profile can be plotted for the given meter configuration and current operating conditions, being these the same configuration and conditions specified for the state estimation routine.

Figure 7 shows an exemplary uncertainty profile obtained from the toy grid, the respective meter configuration comprises one voltmeter at node 1, with 1% uncertainty; and power injection pseudo-measurements at all nodes, except for node 1, with 50% uncertainty.

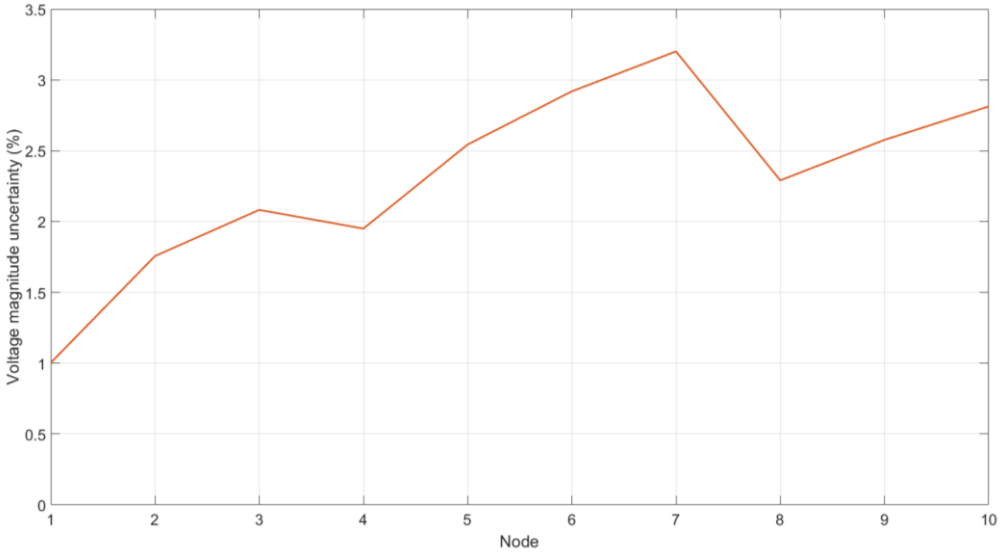

Figure 7. Example uncertainty profile for toy grid.

For the GSA calculations, the same set of inputs are required as in the uncertainty analysis, a given meter configuration, and the results from the state estimation for the current operating conditions.

With these data, N samples are created by sampling within a normal distribution, as explained in Section 3.2, using Latin Hypercube Sampling (LHS) as the sampling strategy for a better filling of the sample space. The number of inputs for the GSA is selected based on the number of meters in the given meter configuration, considering that power meters are treated as two separate inputs, one for active power and one for reactive power. This results in a sample matrix of NxM, where M is the number of the inputs (here, number of voltmeters and twice the number of power injection and power flow meters), and N is the number of samples, at least 1000. With this sample matrix, the state estimation is run N times obtaining Ndifferent voltage magnitude estimates for each node of the grid, which results in a NxN_{Nodes} matrix that is used as output matrix for the GSA.

For running the GSA, the UQLab tool is used [26]. UQLab is an open-source Uncertainty Quantification framework that facilitates performing, among others, sensitivity analysis. For this thesis, the Polynomial Chaos Expansion (PCE) [19] and Sensitivity Analysis (SA) [21] modules are used to perform the GSA of the state estimator. First, the PCE module is used to construct a PCE metamodel from the sample and output matrices described previously, and the type of distribution and parameters used for sampling the input data (Normal, with respective mean and standard deviation). Then, the SA module is used to compute the first and total order Sobol Sensitivity Indices from the constructed PCE metamodel. The sensitivity indices are calculated independently for each voltage magnitude estimate as output and give information on how much the uncertainty of each measurement contributes to the uncertainty of each voltage magnitude estimate. The indexes are then used as inputs for the meter placement methodology explained in the next section.

Figure 8 shows an exemplary heatmap for the toy grid obtained with voltage measurements at all nodes, with 1% uncertainty for node 1 and 3% uncertainty for all other nodes, power injections pseudo-measurements at all nodes, except node 1, with 50% uncertainty; and power flow measurements at all branches with 50% uncertainty, the selection of the meter configuration is explained in section 3.4.1. From the heatmap, the most influential measurements for each of the voltage magnitude estimates are the voltage measurements followed by some of the power flow measurements and then some of the power injection measurements, which is expected for the given meter configuration.

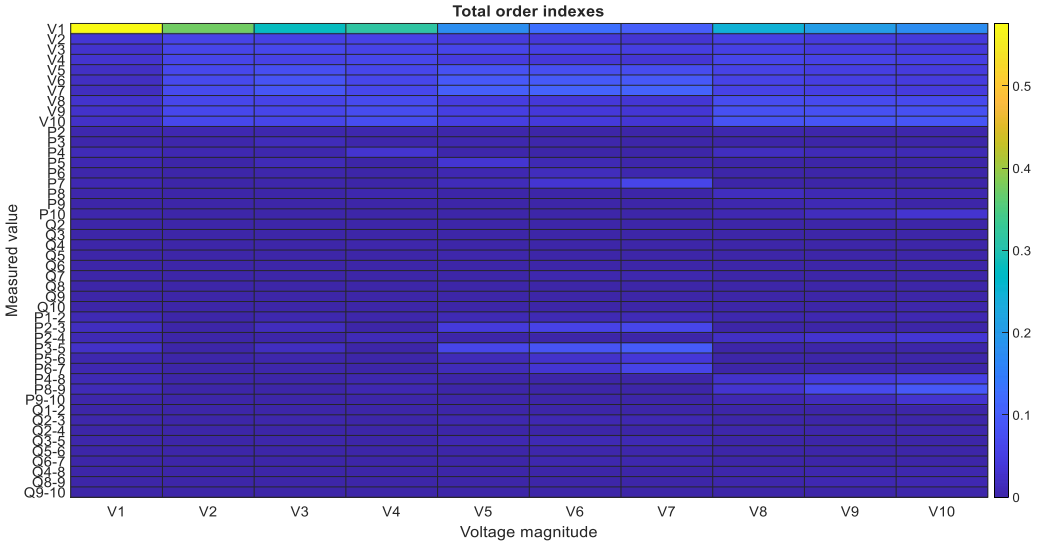

Figure 8. Example of GSA heatmap.

3.4 Meter Placement methodology

A meter placement strategy based on performing GSA of the state estimator is proposed in this thesis as one of the two main components of this work, the other one being the cost-benefit analysis. The objective of this meter placement strategy is to select, based on sensitivity indices, from a pool of possible meters to be installed, the meter that can bring the largest uncertainty reduction to the voltage estimation profile. The use of GSA for the meter placement allows us to consider, at the same time, many uncertainty sources that could affect the state estimation without too high of a computational burden, as well as to analyze in a deeper way how these sources explain the uncertainty of the estimated values. The GSA also provides flexibility regarding the type of uncertain inputs that can be considered, facilitating analysis with different objectives by changing said inputs without major inconvenience to the GSA per se.

3.4.1 Meter configuration setup

The starting point of this strategy is the current meter configuration of the grid. However, the problem setup needs to be different from just the GSA of the state estimator with the given meter configuration, which is not enough to achieve our goal and would be limited to studying which of the meters already present in the grid is the most important, in terms of explaining the variability of the estimates. To achieve our goal, the set of uncertain inputs, as well as their respective uncertainties, considered in the GSA has to be tailored with the ultimate goal of the meter placement in mind. As a first consideration, the current meter configuration cannot be used as it is because it does not include the meters that could be installed, but are not currently present, and therefore these measurements will not be “seen” by the GSA. To make them available to the GSA the meter configuration must include all of the meters that could be installed.

For example, in the toy grid, the initial meter configuration is assumed to be one voltage meter at node 1, with 1% uncertainty, and power injection pseudo-measurements at all nodes, except at node 1, with 50% uncertainty. If the GSA is performed with this configuration, it will not be possible to assess the contribution of, for example, a voltage meter at node 4. Instead, the meter configuration is assumed to be composed of voltage meters at all nodes, power injection pseudo-measurement at all nodes, except at node 1, and power flow meters at all branches.

The inclusion of the meters, or measurements, that are not actually present in the grid raises the question of what uncertainty should be given to them. As a first approach, the uncertainty could be given as the uncertainty that the meter would have if it were present in the grid, for example, 1%, but this brings some problems for the GSA. If voltage measurements are available for the state estimation with very low uncertainty and everywhere in the grid, the estimation is no longer much of an estimation itself and becomes more a measurement of the states, a very unrealistic and not representative case. The state estimation would ignore non-voltage measurements and the magnitude estimates will be very close to the measured value and follow any change in the measurements, as small as it might be, almost entirely. This is a great feature of the state estimator because a

measurement that is considered to be very accurate is very close to the real value. However, for our objective this is not as good because it might create a bias towards the voltage measurements and underestimate all other measurements' importance, not helping to assess the impact that the installation of a particular meter would have.

Figure 9 shows the resulting heatmap of the first-order indices for the toy grid with the assumed meter configuration and using 1% uncertainty for all meters. It could be concluded that the inclusion of a voltage meter is far more important than the inclusion of any power injection or power flow meter. But this would be a wrong conclusion as shown in Figure 10. The figure shows various uncertainty profiles for the toy grid. In red is the profile under the assumed initial configuration, in yellow is the profile after adding a voltage meter at node 2, and in blue is the profile after adding a power flow meter between nodes 3 and 5. Although the addition of the voltmeter, as compared to the power flow meter, is indeed better at reducing the uncertainty profile, the impact of the power flow meter is not negligible as the heatmap would suggest.

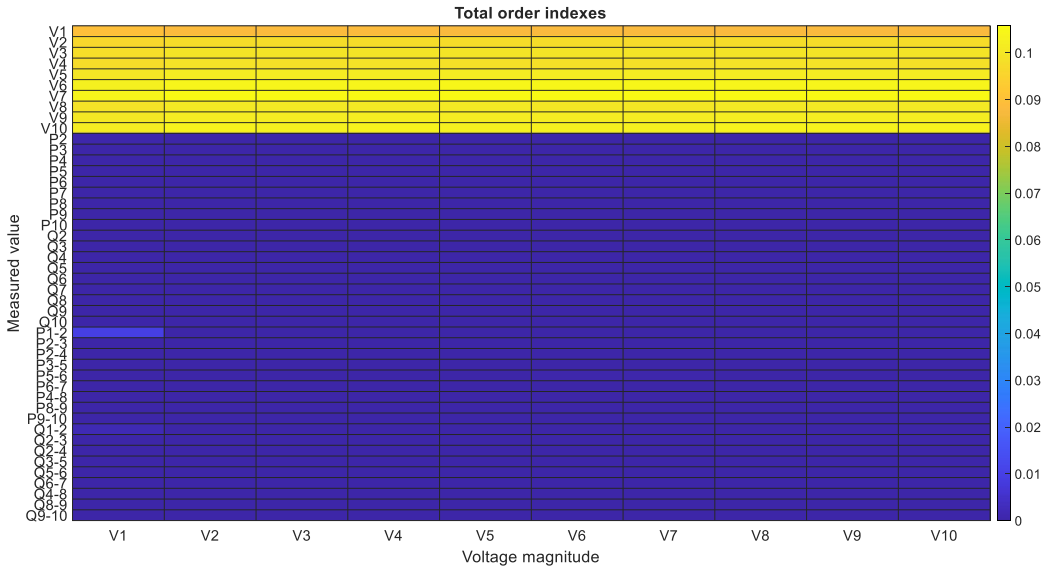

Figure 9. Heatmap assuming 1% uncertainty for all meters – toy grid.

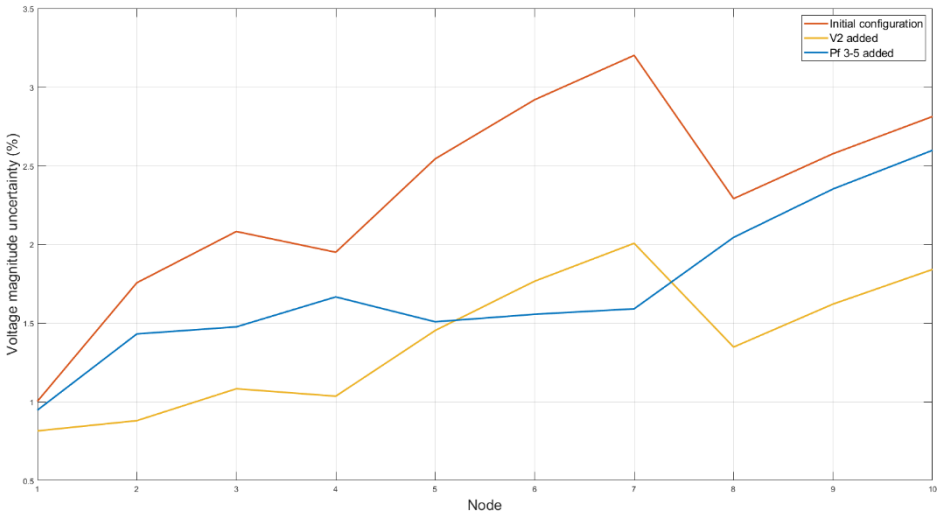

Figure 10. Uncertainty profiles with original meter configuration, with a voltmeter at node 2, and with a power flow meter between nodes 3 and 5.

Another possibility is to consider the uncertainty of the meter that could be installed as a value that does not affect the uncertainty of the state estimation results, but this would also result in misleading sensitivity indices because a measurement with a high uncertainty would just be ignored by the state estimator due to its weighting strategy and would have a very low sensitivity index. Figure 11 shows the resulting heatmap when a high uncertainty is assumed for the meters to be installed, in this case, voltmeters at all nodes are assumed to have 50% uncertainty, except for node 1, whose meter is considered to be present in the initial configuration with 1% uncertainty. Power injection pseudo-measurements are assumed to have 50% uncertainty, as in the initial configuration; and power flow meters are considered to have 500% uncertainty. The heatmap would suggest that the voltmeter at node 1 and a couple of the power injections are the most important measurements. However, Figure 12 shows that, for example, installing a power injection meter at node 7 is not better at reducing the uncertainty profile than installing a voltmeter at node 2 or a power flow meter between nodes 3 and 5.

Uncertainties values should then be selected so that the respective measurement does not become overly dominant or completely ignored by the state estimator weighting. An exact value or a well-defined strategy for choosing the uncertainty values is not provided in this work. Instead, general guidelines are provided to tune these values according to the grid that is used, this process also requires the input of the expertise and knowledge of the grid of the analyst performing the meter placement. A first approach to finding these values is to look for an uncertainty value that creates a “halfway improvement” in the uncertainty profile for a specific meter, one that has a big impact on the uncertainty profile.

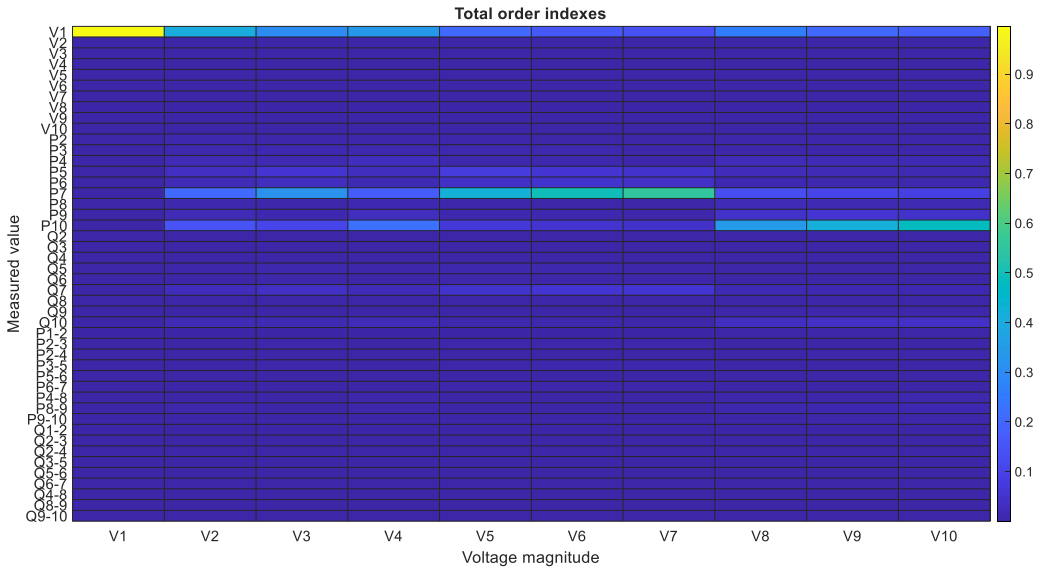

Figure 11. Heatmap assuming 50% uncertainty for voltmeters and 500% uncertainty for power flow meters – toy grid.

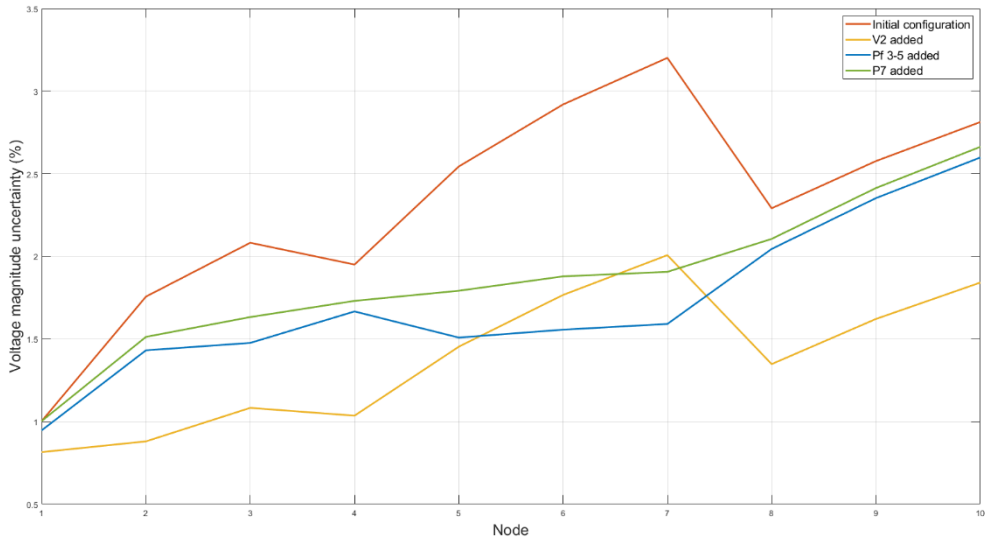

Figure 12. Uncertainty profiles with original meter configuration, with a voltmeter at node 2, with a power flow meter between nodes 3 and 5, and with a power injection meter at node 7.

Figure 13 shows this "Halfway improvement" for a voltmeter installed a node 7. The figure shows the uncertainty profile of the toy grid for different values of uncertainties associated with the measurement, no measurement, 50%, 3%, and 1% uncertainty. From the graph, it can be seen that not having the measurement and having it with an uncertainty of 50% have more or less the same impact on the uncertainty profile, which makes 50% the worst case when this measurement is available, a similar result could be obtained with more or less uncertainty, for example, 25% uncertainty, but the exact uncertainty value at which the worst case occurs is not important, rather the shape of the curve is the important part. The profile when the uncertainty is considered as 1% is the best possible one when this measurement is present, again a similar profile could be obtained with a slightly higher uncertainty, but the important part is the shape of the profile. The profile when the uncertainty is

considered as 3% shows a visual “halfway improvement” in the profile, in the sense that it is more or less in the middle between the worst and best scenarios.

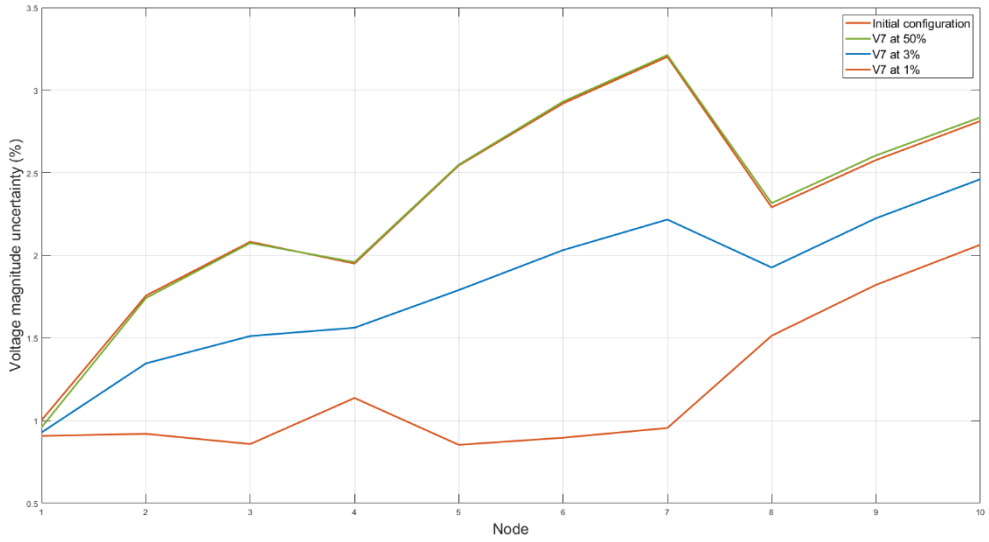

Figure 13. “Halfway improvement” for voltmeter at node7.

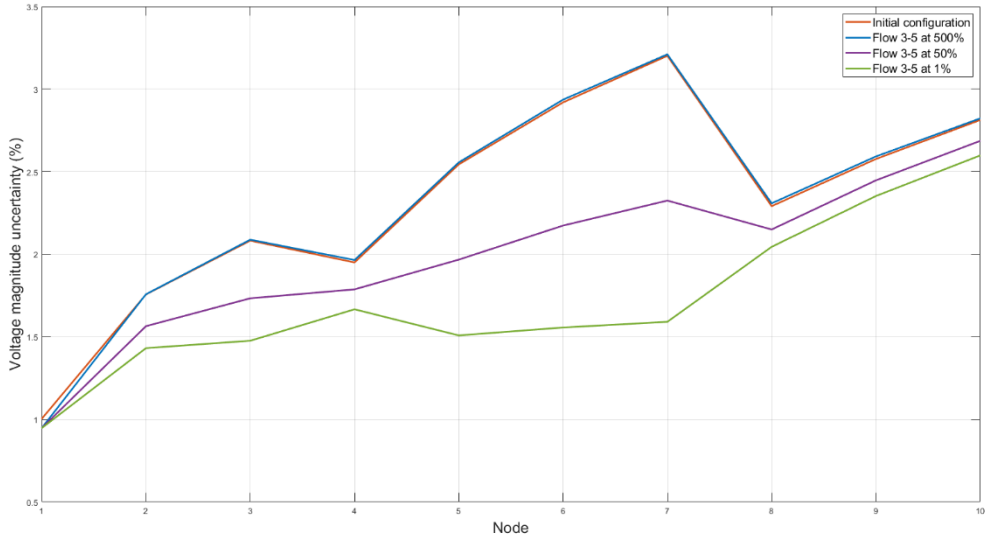

Figure 14. “Halfway improvement” for the power flow meter between nodes 3 and 5.

Figure 14 shows the same graph for the power flow meters in the toy grid. The chosen uncertainty value for the “halfway improvement in this case is 50%. These uncertainty values are then chosen as the uncertainty values to be used in the GSA for the respective type of meter. The best value to be used is not necessarily this 3 or 50%, it could be more or less, but this proved to be a good initial choice. Further ahead in the meter placement procedure, the chosen values should be re-evaluated by comparing the suggestions coming from the meter placement strategy and the analyst’s expertise and knowledge of the grid. One important factor to keep in mind is that the chosen uncertainty values should not be low enough that one type of meter is favored over another by the state estimator just because of its low uncertainty. In such a case, the chosen value should be increased to eliminate the bias towards a specific type of meter. Figure 15 shows the resulting heatmap using 3 and 50% as the

selected uncertainties, power flow meters are now shown to have some importance, not as much as voltage meters, but definitively more than before.

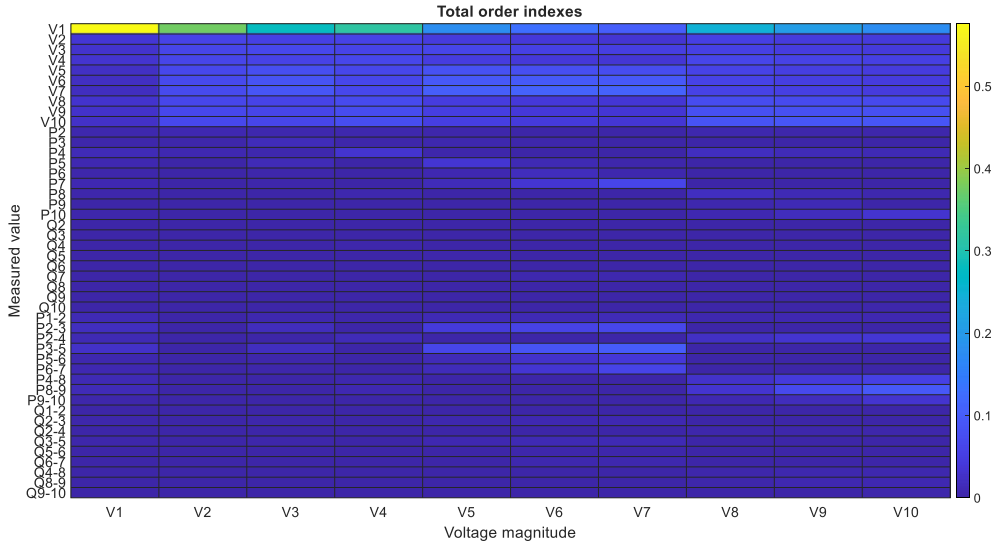

Figure 15. Heatmap of the first-order Sobol' indices with the chosen uncertainty values for the toy grid.

3.4.2 Meter placement procedure

The general procedure for the meter placement is as follows and is summarized in Figure 16:

- Step 1: Define the meter configuration including already present meters and meters that could be installed.
- Step 2: Generate N samples of the measurements given the meter configuration and run N state estimations.
- Step 3: Using the sampled measurements and the results of the state estimation run the GSA of the state estimator and obtain the SIs of each meter, or measurement, for each magnitude estimate.
- Step 4: Based on the SIs choose the most influential meter, or measurement, as corrective action, i.e., install the selected meter.
- Step 5: Update the meter configuration with the suggested corrective action.
- Step 6: Go back to step 2.

Now the problem lies in how to choose the corrective action for step 4. Looking at the sensitivity indices we can see which meter, or measurement, is contributing the most to the uncertainty of a given magnitude estimate. However, since the sensitivity indices are calculated at the node-level and grid-level information is required to make a decision on which meter should be installed, a summary metric based on the indices has to be implemented. The chosen metric has to, on one hand, summarize the SIs of one meter, or measurement, for each of the magnitude estimates into a single value and, on the other hand, reflect the objective of lowering the uncertainty profile. After the summary values for each meter or measurement are obtained, they are sorted in descending order and the highest valued one,

ignoring meters already present in the grid, is chosen as the suggested corrective action, i.e., the meter to be installed. For this work, three metrics were proposed and used for the simulations.

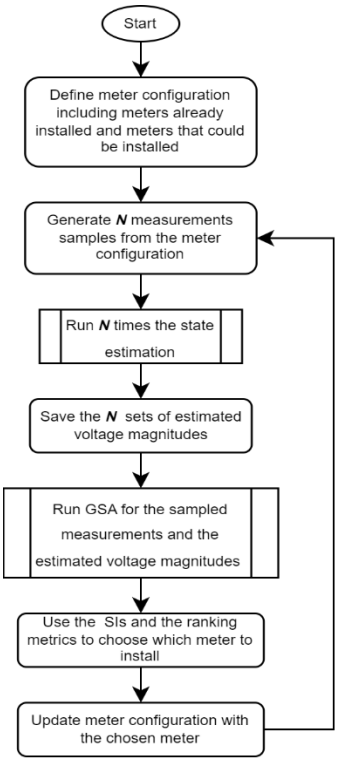

Figure 16. Flowchart for the meter placement strategy.

3.4.3 Metrics for meter placement

Equation (33) shows the first proposed metric, "weighted sum", where Imp_{x_i} is the summarized value given to the meter or measurement x_i; $T_{x_i,j}$ is the total order Sobol index of meter, or measurement, x_i for node j; and $U_{\hat{V}_j}$ is the extended uncertainty in percentage for node j, as in equation (32). This metric takes the sum of the SIs obtained for a meter, or measurement, as a measure of how important they are on a grid-level, and then weights it with the square of the expanded uncertainty. The latter fulfills two different functions, first, it gives an indication of how far the uncertainty of a magnitude estimate is from a completely ideal zero uncertainty, and second, it gives more importance to meters, or measurements that are important to the most uncertain estimates.

$$Imp_{x_i} = \sum_{j=1}^{N_{Nodes}} T_{x_i,j} * U_{\hat{V}_j}^2 \tag{33}$$

Equation (34) shows the second metric, "weighted sum with threshold", where Imp_{x_i} is the summarized value given to the meter or measurement x_i; $T_{x_i,j}$ is the total order Sobol index of meter, or measurement, x_i for node j; and $U_{\hat{V}_j}$ is the expanded uncertainty in percentage for node j, as in equation (32). This metric is very similar to the "weighted sum", but with the difference that it

considers only the SIs of a meter, or measurement, for a given node if the uncertainty of the estimated voltage magnitude for that node is bigger than an arbitrary threshold Thr. This allows to direct the corrective actions to the nodes with higher estimation uncertainties. The threshold also works if the goal of the meter placement is reducing the maximum uncertainty below a given value. In that case, as the uncertainty of a node falls below the threshold, the node will stop being considered in the decision-making process.

$$Imp_{x_i} = \sum_{j=1}^{N_{nodes}} T_{x_i,j} * U_{\hat{V}_j}^2, \qquad for\ U_{\hat{V}_j} > Thr \tag{34}$$

Equation (35) shows the third metric, "weighted sum for one feeder". Where Imp_{x_i} is the summarized value given to the meter or measurement x_i; f is the feeder in which the node with the highest estimation uncertainty is; $T_{x_i,j}$ is the total order Sobol index of meter, or measurement, x_i for node j; and $U_{\hat{V}_j}$ is the expanded uncertainty in percentage for node j, as in equation (32). This metric is also similar to the previous ones, but instead of having a grid-level focus, it has a feeder-level focus. This is because the benefits in the uncertainty profile obtained by the installation of a single meter are almost completely local to the feeder in which the meter is installed, at least for feeders with a moderate number of nodes, and this allows for a stepwise uncertainty reduction of peaks in the uncertainty profile.

$$Imp_{x_i} = \sum_{f} T_{x_i,(j \in f)} * U_{\widehat{V_{j \in f}}}^2 \tag{35}$$

Other metrics were tested during the work of this thesis but did not perform very well. Among these were variations of the proposed metrics, like not focusing on the feeder with the highest uncertainty, but on the feeder with the highest sum of uncertainties. This, however, might focus the suggestions on feeders with a higher number of nodes, but low uncertainty, and ignore feeders with a lower number of nodes, but high uncertainties. Another proposition was to focus the weighted sum on a selection of nodes based on the local maxima of the uncertainty profile, but this option loses performance as the uncertainty profile goes lower since many local maxima start to appear altering the focused approach. A somewhat different approach was to sort the SIs for each node, and the choosing as corrective action the meter associated with the SI that was sorted as the highest the most times, i.e., the mode. This approach also did not perform very well in comparison to the three presented here above.

3.4.4 Meter placement in the toy grid

For a better understanding of the meter placement strategy the first three iterations for the toy grid are shown next following the “weighted sum” metric, the rankings for the other two metrics will also be shown but ignored. For the weighted sum with threshold, the threshold was selected as 1%.

The initial meter configuration consists of a voltage meter at node 1 with 1% uncertainty and power injection pseudo-measurements at all nodes, except node 1, with 50% uncertainty, resulting in the uncertainty profile shown in Figure 17. Now for the meter placement, all meters that could be installed are added to the meter configuration. This means that we have voltage meters at all other nodes with 3% uncertainty, and power flow meters at all branches with 50% uncertainty, which results in the heatmap in Figure 18. From these SIs, the three metrics are computed, and the first ten ranked results are shown in Table 2.

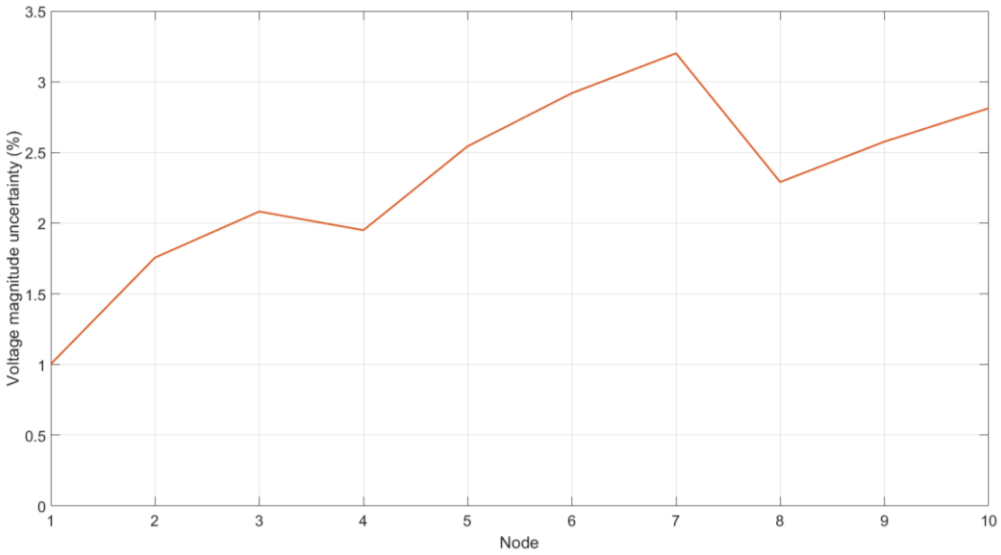

Figure 17. Initial uncertainty profile for the toy grid.

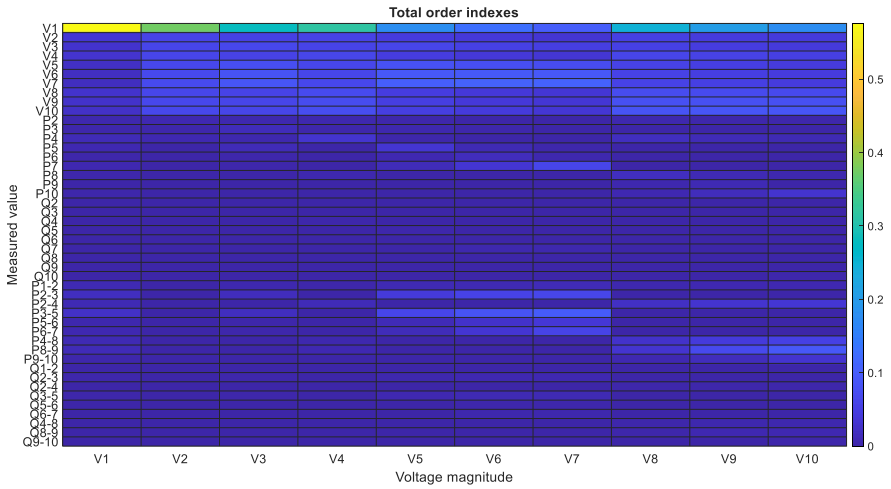

Figure 18. Initial configuration heatmap for toy grid.

Table 2. Ranked metrics for initial meter configuration in toy grid.

Weighted sum		**Weighted sum with threshold ($\boldsymbol{Thr = 1\%}$)**		**Weighted sum for one feeder**	
V1	11.5299	**V1**	11.5299	**V1**	4.5271
V7	*4.6141*	***V7***	*4.6141*	***V7***	*3.1059*
V6	4.2459	**V6**	4.2459	**V6**	2.7525
V5	3.7479	**V5**	3.7479	**V5**	2.2855
V10	3.6002	**V10**	3.6002	**P3-5**	2.1915
V9	3.4203	**V9**	3.4203	**V3**	1.6840
V8	3.2009	**V8**	3.2009	**P2-3**	1.4959
V3	3.1010	**V3**	3.1010	**V10**	1.3419
V4	2.8839	**V4**	2.8839	**V9**	1.3283
V2	2.6296	**V2**	2.6296	**V8**	1.3220

From the table, the suggested meter to install is a voltmeter at node 7, we ignore the voltmeter at node 1 because it is already present in the grid. Figure 19 shows how the uncertainty profile changes when installing each of the first three suggested meters, it can be seen that the inclusion of a voltmeter at node 5, ranked 4th, has the lowest impact of the three and that the inclusion of a voltmeter at node 7 or 6, ranked 2nd and 3rd, respectively, has very similar results, this as expected from the ranking, see the similar values for V7 and V6, and the somewhat lower value for V5.

Figure 20 shows how the uncertainty profile changes after the addition of a voltmeter at node 7, the suggested meter, the figure also shows what the profile would look like if a voltmeter at node 2 and a power flow meter between nodes 9 and 10 were installed. The resulting profiles are in agreement with the ranking as the voltmeter at node 7, which is ranked 2nd, brings an important reduction of the uncertainty profile; the voltmeter at node 2, which is ranked 10th, also results in a good reduction in the profile, yet not as good as the voltmeter in node 7; and lastly, the power flow meter between nodes 9 and 10, which is ranked 23rd, does not produce a significant reduction in the profile. This comparison between higher and lower-ranked meters is only done to show that the ranking makes sense and will be omitted in the following for the sake of brevity.

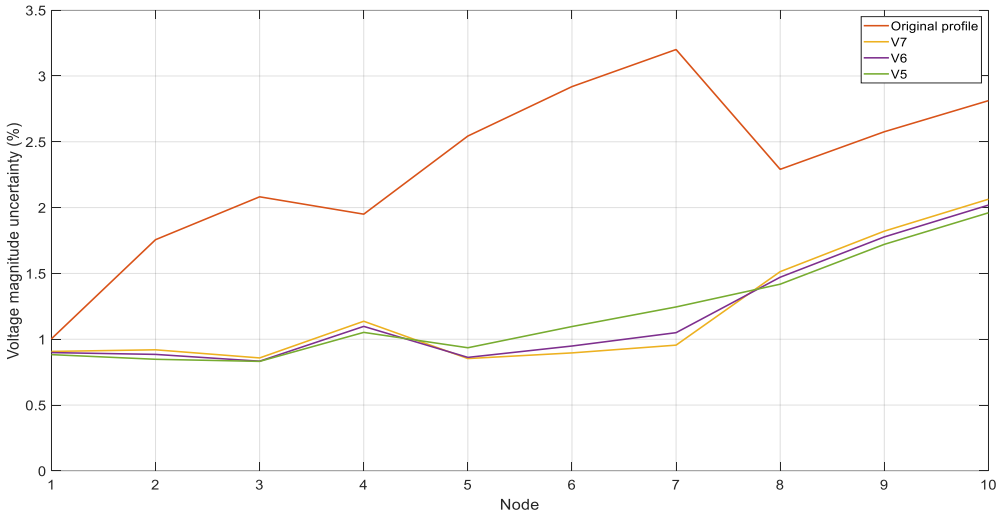

Figure 19. Comparison of the first three ranked meters.

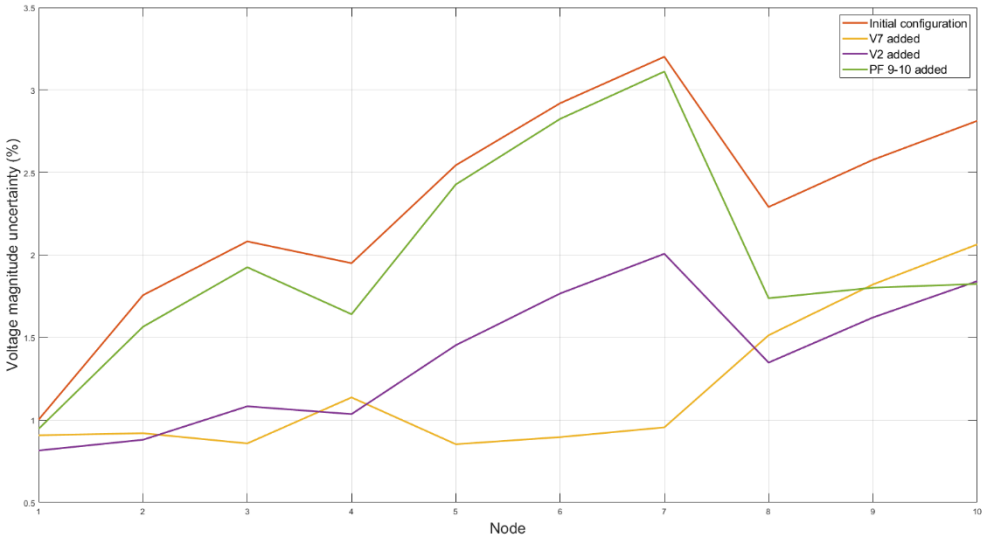

Figure 20. Possible uncertainty profiles after first corrective action.

After having decided to install a voltmeter at node 7 as the corrective action, we now update the meter configuration and run the GSA again. This produces the heatmap shown in Figure 21 and the ranking shown in Table 3. From the table, the suggested corrective action is to install a power flow meter between nodes 8 and 9. Figure 22 (note the change in the limits of the axis showing the uncertainty) shows the resulting uncertainty profile after installing the suggested meter, a voltmeter at node 2, which is ranked 9th, and after installing a power flow meter between nodes 1 and 2, which is ranked 27th. It is worth noting that, as the levels of uncertainty decrease, the differences in the corrective actions become less and less evident.

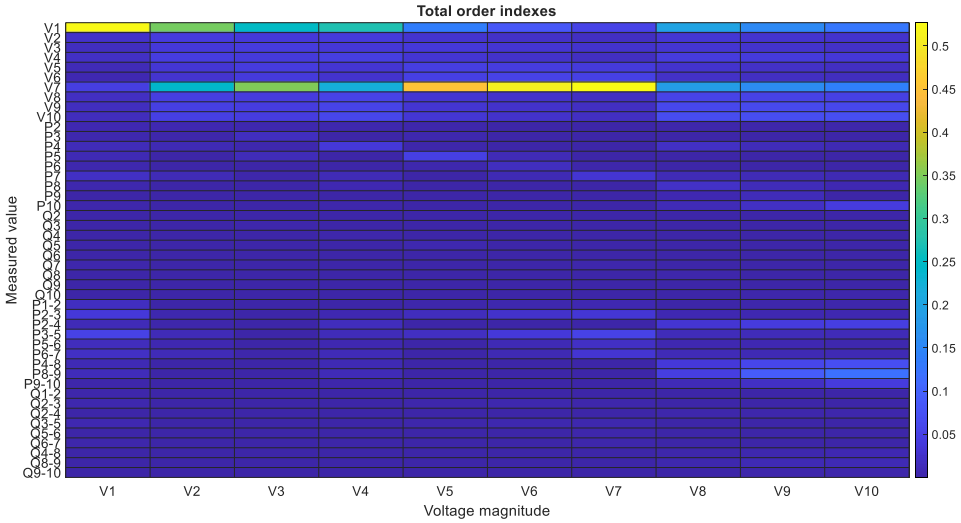

Figure 21. Heatmap for toy grid after first corrective action.

Table 3. Ranked metrics after first corrective action in toy grid.

Weighted sum		**Weighted sum with threshold ($Thr = 1\%$)**		**Weighted sum for one feeder**	
V7	3.5607	**V1**	1.8655	**V1**	1.8651
V1	2.9879	**V7**	1.8379	**V7**	1.8375
Pf8-9	*0.9488*	***Pf8-9***	*0.9338*	***Pf8-9***	*0.9367*
V10	0.9095	**V10**	0.7588	**V10**	0.7589
V9	0.8275	**V9**	0.6784	**V9**	0.6780
V8	0.7241	**Pf4-8**	0.6041	**Pf4-8**	0.6043
Pf4-8	0.6136	**V8**	0.5759	**V8**	0.5754
V4	0.5880	**V4**	0.4411	**V4**	0.4411
V2	0.4925	**Pf 2-4**	0.4280	**Pf 2-4**	0.4280
V3	0.4696	**V2**	0.3489	**V2**	0.3487

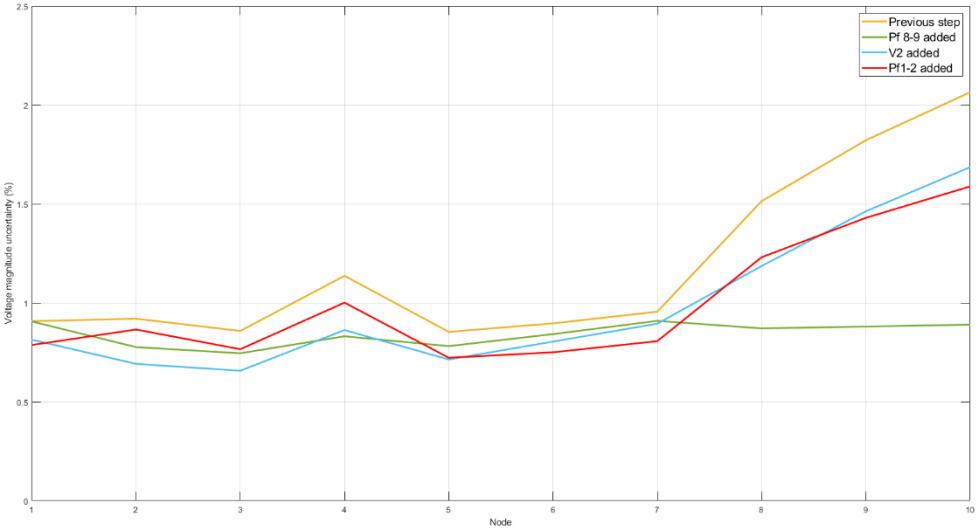

Figure 22. Possible uncertainty profiles after the second corrective action.

With the power flow meter between nodes 8 and 9, the meter configuration can be updated, and a third round of the meter placement can be done. This results in the heatmap shown in Figure 23 and the ranking shown in Table 4. From the table, the suggested corrective action is to install a voltmeter at node 10. Figure 24 (note the change in the limits of the axis showing the uncertainty) shows the resulting uncertainty profiles for installing a voltmeter at node 10, ranked 3rd, and the suggested action; installing a voltmeter at node 6, ranked 8th (but the suggested action by the third metric); and installing a power flow meter between nodes 1 and 2, ranked 23rd.

As expected, the power flow meter is not as good as the other options, but it is worth noting the difference between metric 1 and metric 3, which up to this point had agreed on the suggested meter. The difference comes from the different objectives of the metrics, since metric 3 looks at the feeder where the node with the highest estimation uncertainty is, which in this case is feeder 1, the suggested corrective action is expected to mostly improve the uncertainties of the nodes in this feeder. Indeed, if we compare the two profiles, we see that the uncertainties of the nodes in feeder 1, nodes 3, 5, 6, and 7, are lower when we follow metric 3. At this point, judging one over the other becomes more a matter of the purpose of the metric. The previous shows the influence of the chosen metric in the meter placement results, metrics with different objectives will suggest different actions.

It is also worth noting that metric 2 produces no ranking since all the uncertainties are below the selected threshold, 1%, as shown in Figure 22, and by its definition, it has completed its purpose.

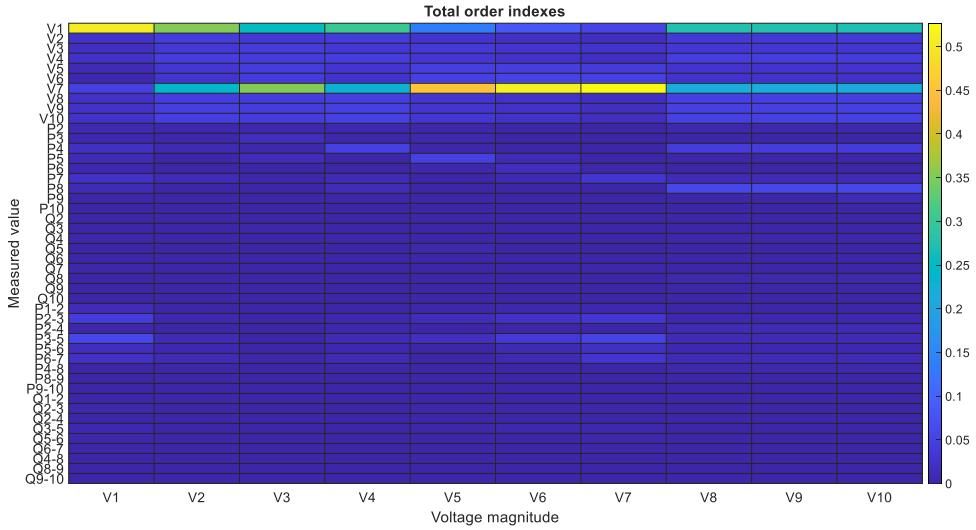

Figure 23. Heatmap for toy grid after second corrective action.

Table 4. Ranked metrics after the second corrective action in the toy grid.

Weighted sum		Weighted sum with threshold ($Thr = 1\%$)		Weighted sum for one feeder	
V7	2.1145	**V1**	-	**V7**	1.2695
V1	1.8024	**V2**	-	**V1**	0.3283
V10	*0.2749*	***V3***	-	***V6***	*0.1306*
V9	0.2709	**V4**	-	**V5**	0.1149
V8	0.2679	**V5**	-	**V3**	0.0910
V4	0.2544	**V6**	-	**Pf3-5**	0.0817
V5	0.2374	**V7**	-	**V10**	0.0791
V6	0.2367	**V8**	-	**V9**	0.0783
V2	0.2367	**V9**	-	**V8**	0.0775
V3	0.2367	**V10**	-	**V4**	0.0757

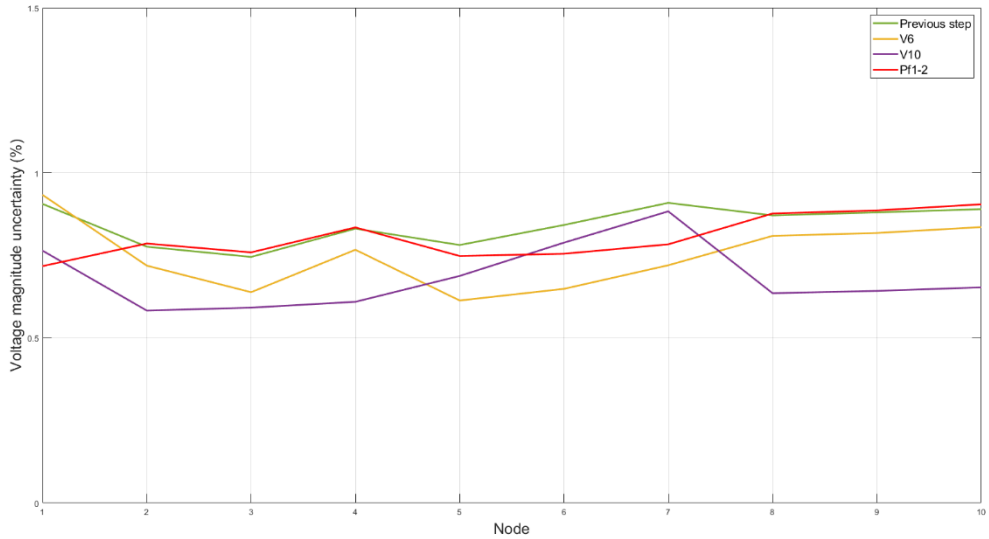

Figure 24. Possible uncertainty profiles after the third corrective action.

3.5 Cost-Benefit Analysis

The second part of this thesis is the implementation of a cost-benefit analysis comparing the yearly cost of installing a new meter in the grid, to improve the state estimation, versus the savings in the yearly cost of flexible power required by a state estimation-based voltage control. The savings come from the improvement that the considered meter brings to the accuracy of the state estimation results and, consequently, on the reduction of the safety margins considered in the voltage control algorithm.

3.5.1 State estimation-based voltage control

The state estimation-based voltage control, as explained in section 2.3.2, is used to compute the change in the power output setpoints of flexible power sources that is required to keep all the voltage magnitudes within desired limits. For computing these changes an optimization algorithm takes as input a set of voltage magnitudes and respective uncertainties, one for each voltage magnitude, and a pool of available flexible power sources, with respective set point limits, whose power set points may be potentially changed.

The voltage magnitudes are obtained from a power flow computation considering the current operating conditions, the uncertainties are computed by making use of the state estimation routine as explained in section 2.3.2, considering the current meter configuration, and are used to restrict the desired voltage range. This restricted voltage range then ensures that the corrected voltage magnitudes remain within limits even if the actual voltage deviates from the estimated one, as explained in section 2.4.

3.5.2 Cost-benefit analysis

For the yearly cost-benefit analysis, first, the total amount of flexible power requested in a year, and its respective cost considering an initial meter configuration, is needed. For this, the generation and load profiles for the Atlantide network are used. These profiles provide a 15-minute resolution for the simulation and allow us to adapt accordingly the limits for the maximum and minimum power that can be delivered by the pool of flexible sources by scaling the operating set points in those instants of time where the voltage exceeds the allowed limits. Besides the PV, Wind, and CHP resources available in the grid, Energy Storage Systems are assumed to be installed at each node where a PV plant is present, see Figure 6. After the voltage control algorithm has been executed at each time step in the year, the overall requested power is computed by adding the magnitude of each set point change at each time step for all the flexible sources, then the respective cost is computed by multiplying the total requested power by a given cost of flexible power.

Secondly, for the cost comparison, a list of meters to be considered is needed. From this list, meters are selected iteratively to update the initial meter configuration. Then, the year simulation is done again to obtain the yearly cost of flexible power, considering the modified meter configuration with the additional meter. If the yearly cost of the meter is lower than the savings due to its installation, i.e., the difference in yearly flexible power cost with and without the meter, then the installation of

the meter is cost-convenient. If the cost of the meter is higher, then its installation is not cost-convenient. The installation of a meter reduces the amount of requested flexible power since its installation reduces the uncertainty profile of the voltage magnitude estimates, which makes the modified voltage limits, used as inputs to the voltage control algorithm, less stringent. If the installation of the considered meter is advised, then the process is repeated with the next meter in the list until a meter is found whose yearly cost is higher than the savings from its installation.

If during the year simulation, the uncertainty of any estimated magnitude surpasses a value of 5% at any time step, the lower voltage limit becomes higher than the upper voltage limit, for example, at 6% uncertainty the lower and upper limits are 1.01 and 0.99 p.u., respectively, following (28) and (29)**Error! Reference source not found.Error! Reference source not found.**. In such a scenario, the voltage control algorithm cannot find a solution to the optimization problem since the limits make it impossible. For the Cost-Benefit analysis loop, this is interpreted as the fact that the next meter must be installed, the current year simulation is stopped at this time step and the analysis continues by updating the meter configuration with the next meter and running the year simulation with the updated meter configuration.

The list of meters used for this analysis is obtained by repeating several times the GSA-based meter placement strategy explained in Section 3.4. This list makes then the connection between the two main parts of this thesis. It is worth noting that the two parts are independent of one another and that a different meter placement strategy could be used to obtain the list of meters to consider without affecting the cost-benefit analysis framework. The cost-benefit analysis loop is summarized in the flowchart shown in Figure 25.

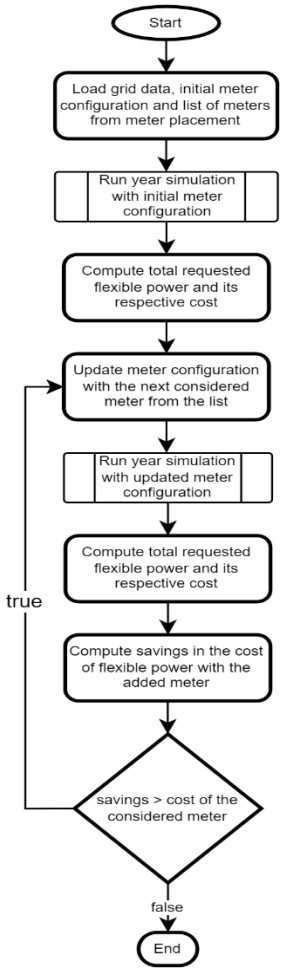

Figure 25. Flowchart for the cost-benefit analysis.

4 Results and Discussion

This chapter shows the results obtained from the different simulations that were done for this thesis. Section 4.1 focuses on the results obtained from the meter placement strategy for the Atlantide grid, and Section 4.2 shows the resulting Cost-benefit analysis results obtained from the corresponding meter placement results.

4.1 Meter placement results

For the meter placement strategy, the Atlantide grid was always assumed to have an initial meter configuration comprising one voltmeter at node 1, with 1% uncertainty; and power injection pseudo-measurements at all nodes, except node 1, with 50% uncertainty. For the GSA and SIs computation, it was assumed that voltmeters could be added at any other node, as well as power flow meters at any branch. The uncertainty used to run the GSA for the meters that could be installed was 3% for voltage meters and 50% for power flow meters, and the uncertainty considered when a meter was installed was 1% for voltage meters and 2% for power flow meters. The simulations were run on a computer with Windows 10 and an AMD Ryzen 5 3550H with Radeon Vega Mobile Gfx@2.10 GHz processor, the computational time for the calculation of the PCE and the Sensitivity Indices for one round of the meter placement and 1000 samples (with 295 inputs and 99 outputs) took around 93.2 seconds for the Atlantide grid.

4.1.1 Operating conditions selection

Since there are many different operating conditions available, thanks to the load and generation profiles of the Atlantide network, a representative operating condition, or set of representative operating conditions, must be chosen before the meter placement can be applied. The chosen year must match the year chosen for the cost-benefit analysis loop, in this case, 2030, but which specific time step, or time steps, within the year, remains a degree of freedom.

The grouping of the time steps was done by looking at each respective voltage magnitude profile. For this, a power flow was run at each time step considering the 15-minute profiles. This results in 96*365=35040 different voltage profiles, for the year 2030, to be grouped. For the grouping of the profiles a simple clustering technique was used, the k-medoids method [27]. This method divides all the available profiles into k groups and assigns to each group a centroid within the dataset, the reason why it was chosen over other methods like k-means, where the centroid might not exist in the dataset. Each group contains all the profiles that are closer, given a distance metric, to the centroid of the group than to the centroid of any other group. Figure 26 shows the resulting voltage profiles selected as centroids for 6 clusters, additionally, it shows the profiles where the highest overvoltage (OV) and the lower undervoltage (UV) of the year occur. Since all the selected centroids are basically scaled versions of the profiles with the worst OV and UV, these two were selected as representative profiles. At the time steps of the worst OV and UV, the requested power determined by the voltage control algorithm will be higher since the voltage magnitude are the furthest away from the desired limits. Section 4.1.2

shows the results obtained when only considering the OV case, and Section 4.1.3 shows the results obtained by combining the OV and UV cases.

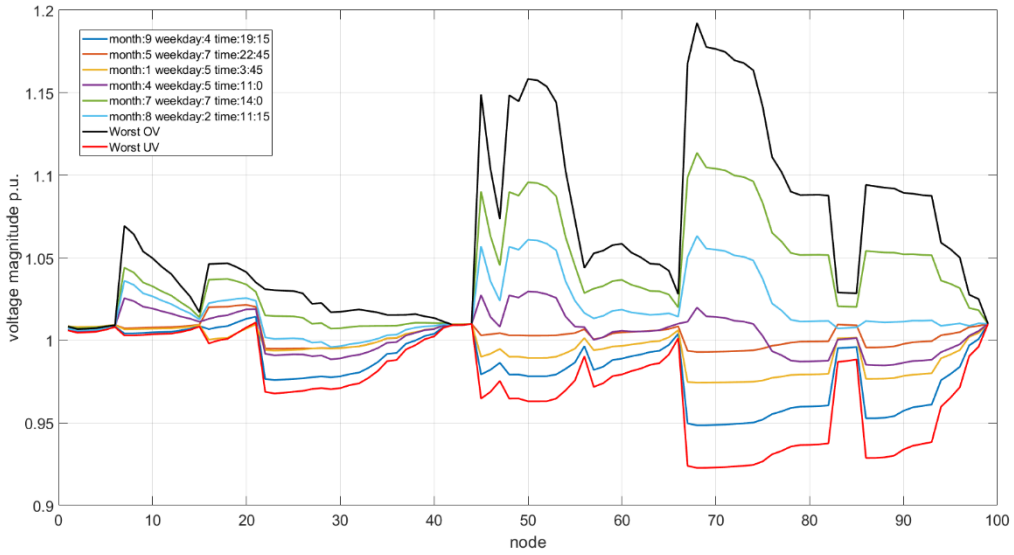

Figure 26. Centroids for 6 clusters.

4.1.2 Meter placement for the OV case

With the selected representative time step and the meter configuration explained at the beginning of Section 4.1 we can start the meter placement procedure. Figure 27 shows the initial uncertainty profiles for the Atlantide industrial grid at the worst OV case. For the simulations, 10 iterations of the meter placement strategy were done to have a large enough list of meters ready to perform the Cost-Benefit Analysis without needing to do additional rounds of the meter placement, for the sake of explaining the results. In practice, doing one round of the meter placement and then one round of the CBA with the single proposed meter will avoid running unnecessary meter placement rounds, which can be very time-consuming depending on the size of the grid and the number of inputs considered. The heatmaps obtained from the first round of the meter placement are shown in Figure 30 and Figure 29 for the OV case. The heatmaps were divided into only voltage and active power flow meters for visualization purposes and because the other meters were not as important.

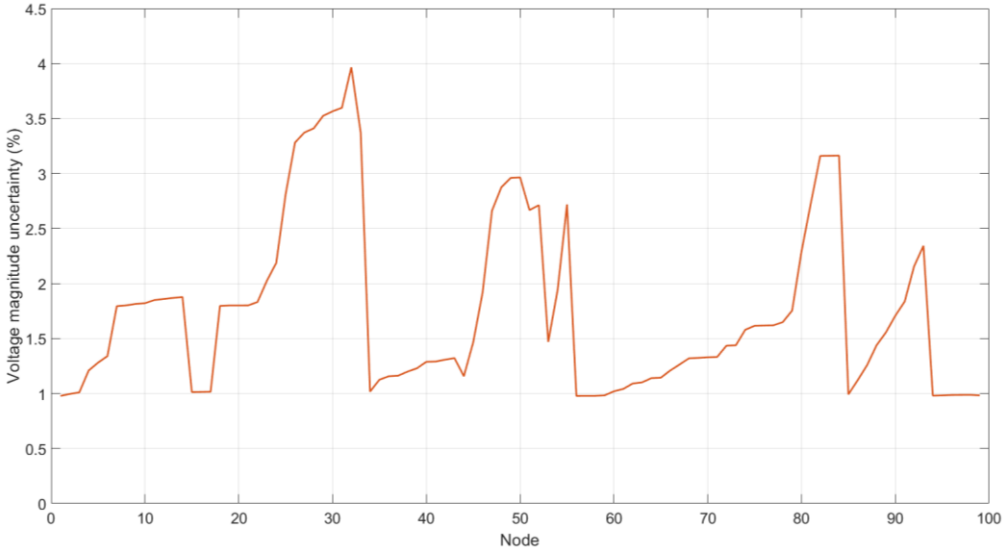

Figure 27. Initial uncertainty profile for worst OV case.

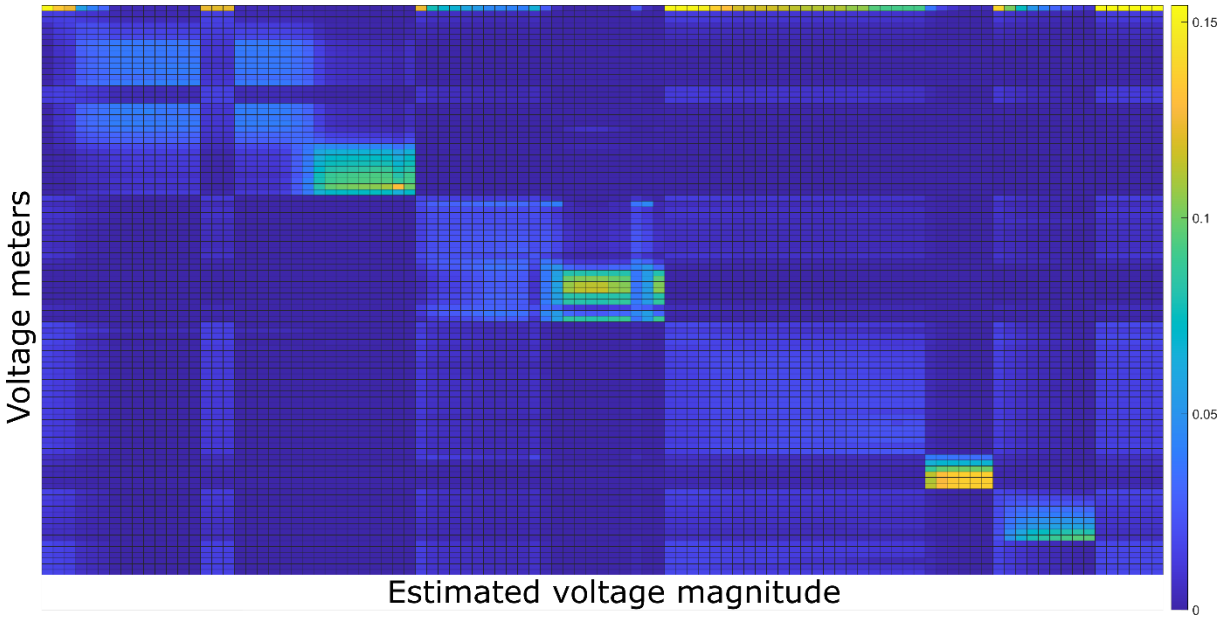

Figure 28. Heatmap for voltage meters – OV case.

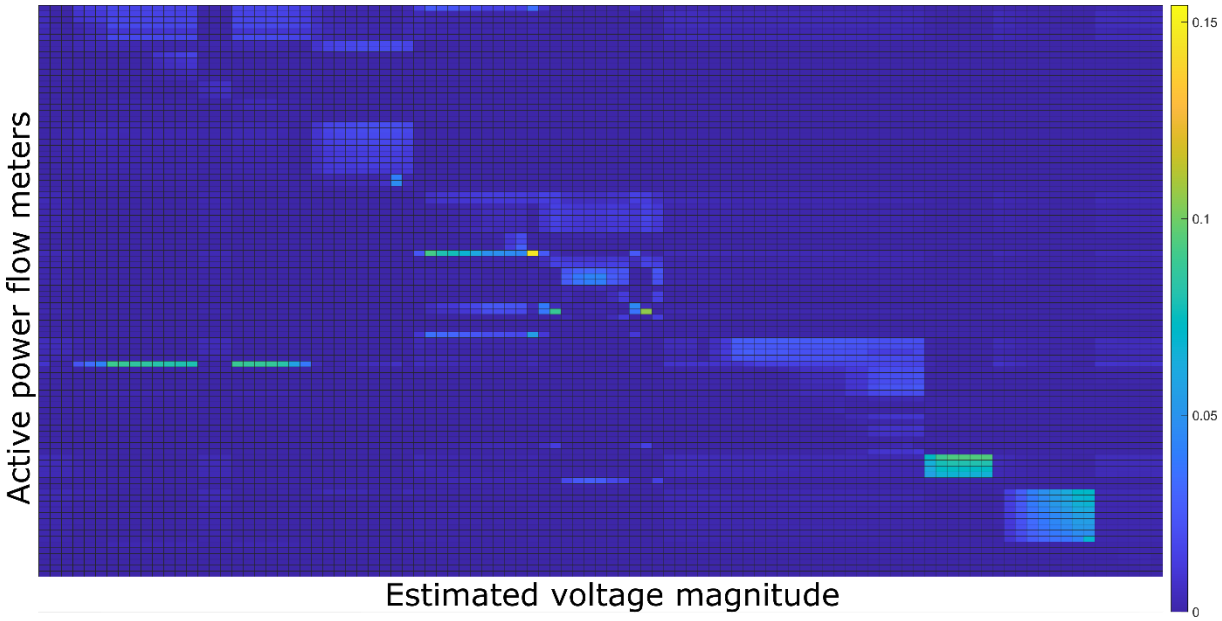

Figure 29. Heatmap for active power flow meters – OV case.

With the intention of showcasing the differences between the proposed metrics, and one that was considered, but did not perform well, an additional metric was used. This additional metric, "modified weighted sum for one feeder", is a modified version of the weighted sum for one feeder, where the feeder for which the weighted sum is done is not the feeder with the highest uncertainty, but the feeder with the highest sum of uncertainties. Table 5 shows the ten suggested meters by each of the four metrics, for the "Weighted sum with threshold" metric a threshold of 1% was used. Figure 30, Figure 31, Figure 32, and Figure 33 show the uncertainty profiles after adding each of the suggested meters by the four metrics.

Table 5. First ten meters suggested by the four metrics.

Weighted sum	Weighted sum with threshold ($Thr = 1\%$)	Weighted sum for one feeder	Modified weighted sum for one feeder
V32	*V32*	*V32*	*V32*
V49	*V49*	*V84*	*V84*
V84	*V82*	*V49*	*V49*
V93	*Pf 62-63*	*V93*	*V93*
Pf 62-63	*V93*	*Pf 1-59*	*Pf 1-59*
V7	*V14*	*V77*	*V77*
Pf 35-44	*V77*	*Pf 62-63*	*Pf 62-63*
V70	-	*V7*	*V7*
Pf 1-85	-	*Pf 35-44*	*Pf 35-44*
V50	-	*Pf 1-85*	*Pf 1-85*

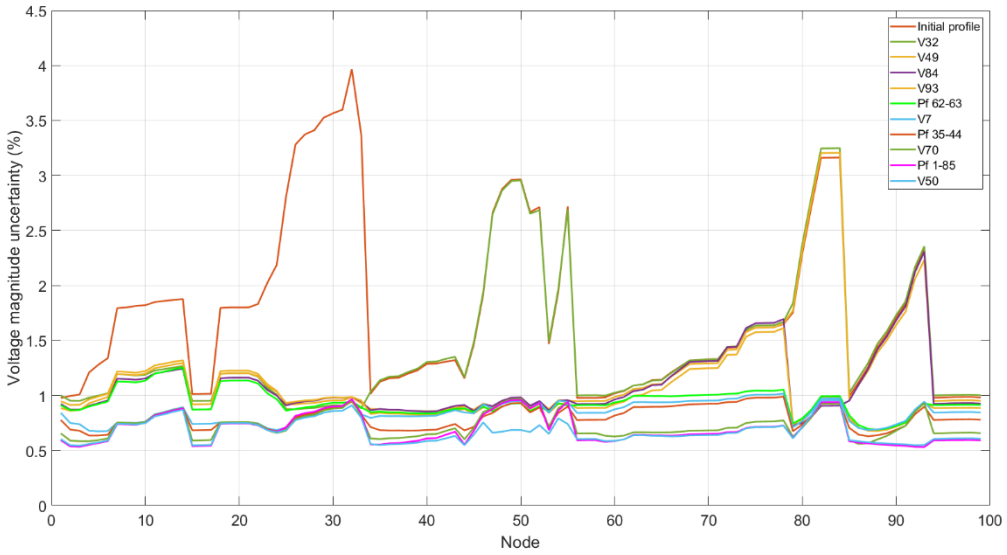

Figure 30. Resulting uncertainty profiles – weighted sum.

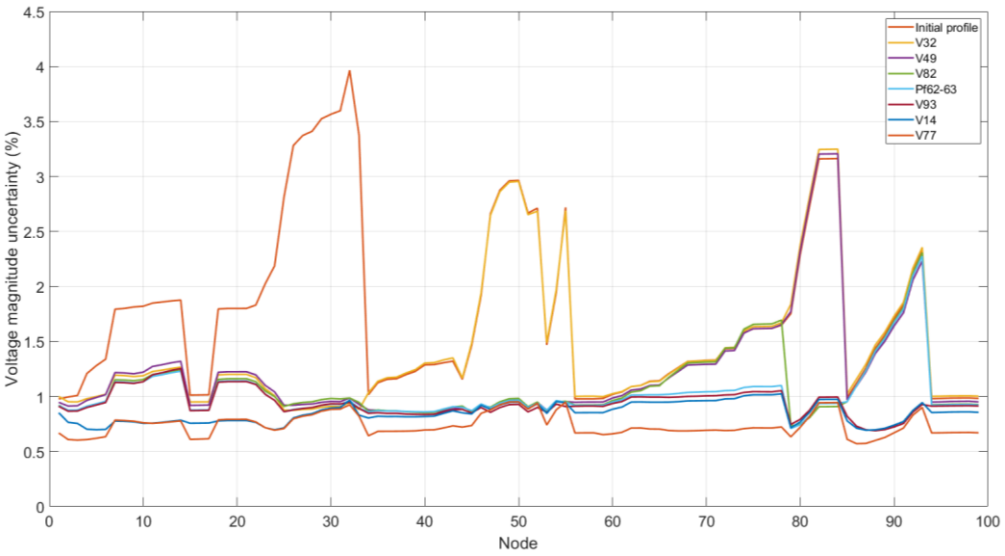

Figure 31. Resulting uncertainty profiles – weighted sum with threshold.

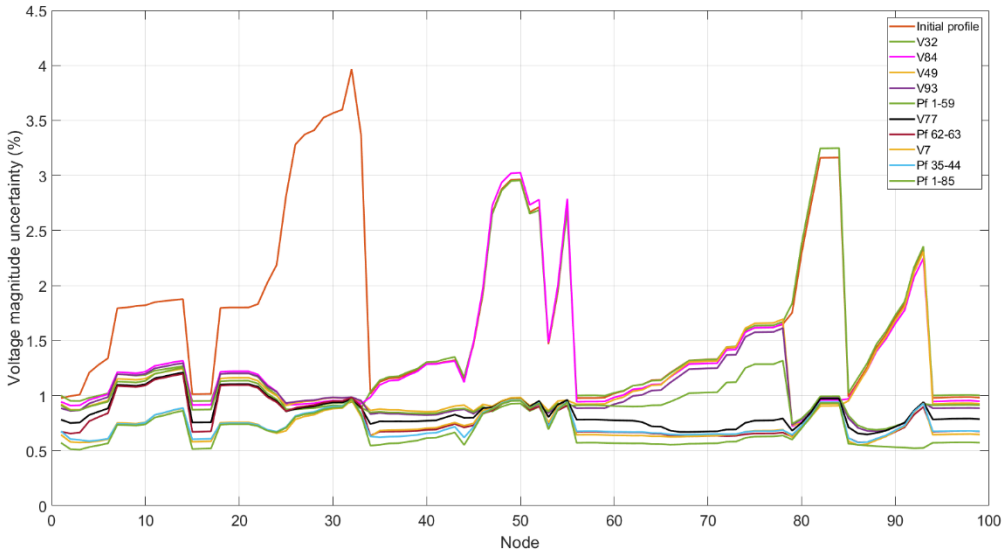

Figure 32. Resulting uncertainty profiles – weighted sum for one feeder.

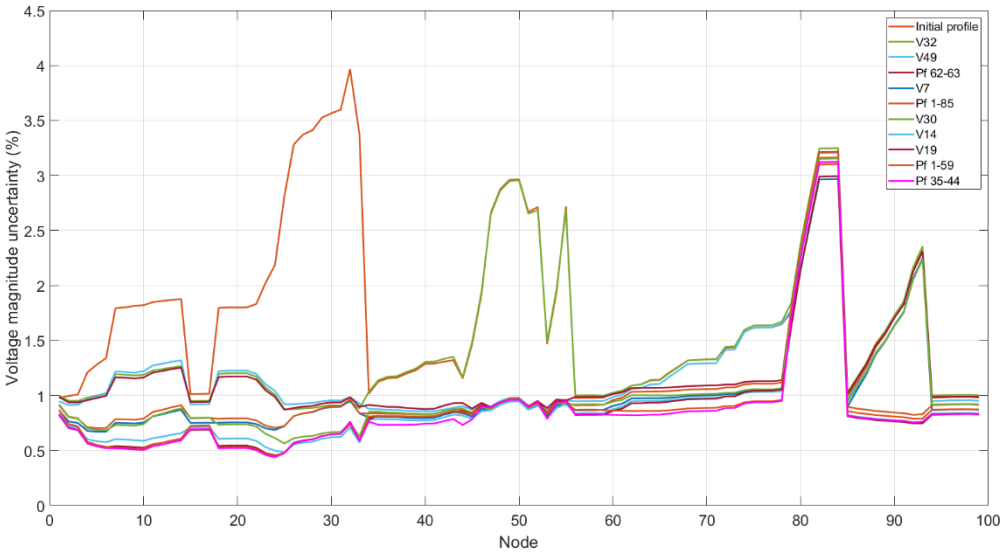

Figure 33. Resulting uncertainty profiles – modified weighted sum for one feeder.

The first thing to note from these results is that the fourth metric, as explained briefly in Section 3.4.3, does not have a good performance because the metric focuses on a feeder with a large number of nodes with low uncertainty, feeder 1 in this case (nodes 2-33), and ignores a feeder with a low number of nodes with high uncertainty, feeder 5 in this case (nodes 79-84). This can be seen in Figure 33, where even after 10 meters, the uncertainties on feeder 5 never changed and 5 of the 10 suggestions are meters placed in feeder 1 (V32, V7, V30, V14, and V19). Different results can be seen for metrics one to three, where a voltmeter, V84, is recommended for feeder 5.

Another thing to notice is that metrics 1 and 2, being very similar, have the same first two suggestions, they differentiate from each other when enough estimation uncertainties fall below the considered threshold. Another differentiating factor for metric 2 is that only seven meters can be suggested, this is because, after the seventh step, all the uncertainties fall below 1%. This, for now, is no indication that the metric is better or worse than the others, that is to be decided in the Cost-Benefit Analysis. To have a clearer look at the end state of the uncertainty profiles, Figure 34 shows the initial profile and the profiles for each metric after 10 steps (7 steps for metric 2).

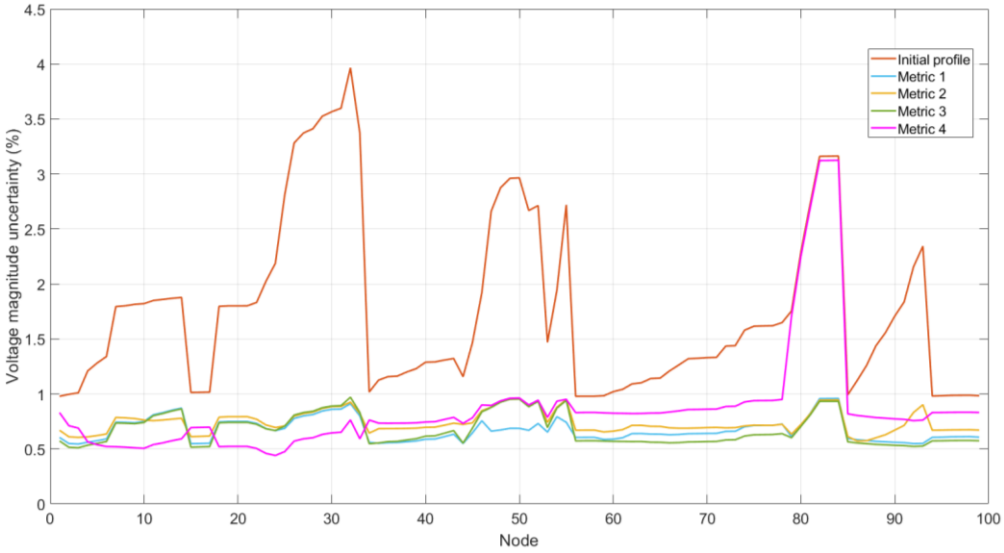

Figure 34. Uncertainty profile after 10 steps for each metric.

4.1.3 Meter placement for combined cases

With the selected representative time steps, OV and UV cases, and the meter configuration explained at the beginning of Section 4.1 we can start the meter placement procedure. Figure 35 shows the initial uncertainty profiles for the Atlantide industrial grid at the worst OV and UV. Before proceeding with the meter placement, a way of putting together the ranking metrics needs to be decided. This is done by computing the metrics individually for the OV and UV cases and adding them. In this case, the resulting importance given to, for example, a voltmeter at node 5, is the sum of the importance given to the meter in each case. For the simulations, only 10 meters were obtained from the meter placement strategy.

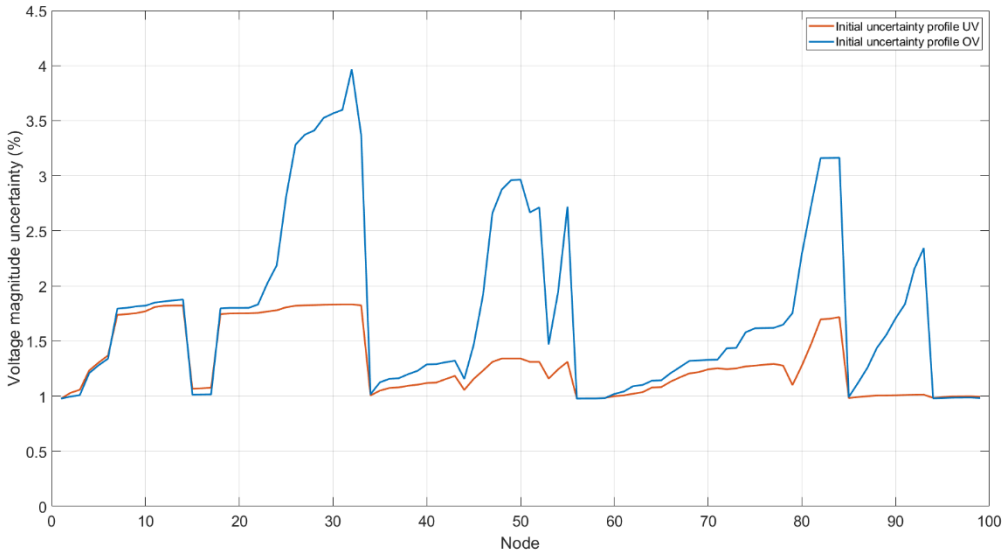

Figure 35. Initial uncertainty profile for worst OV and UV cases.

The heatmaps obtained from the first round of the meter placement for the OV case were shown in Figure 28 and Figure 29. Figure 36 and Figure 37 show the heatmaps for the UV case. The heatmaps were divided into only voltage and active power flow meters for visualization purposes and because the other meters were not as important.

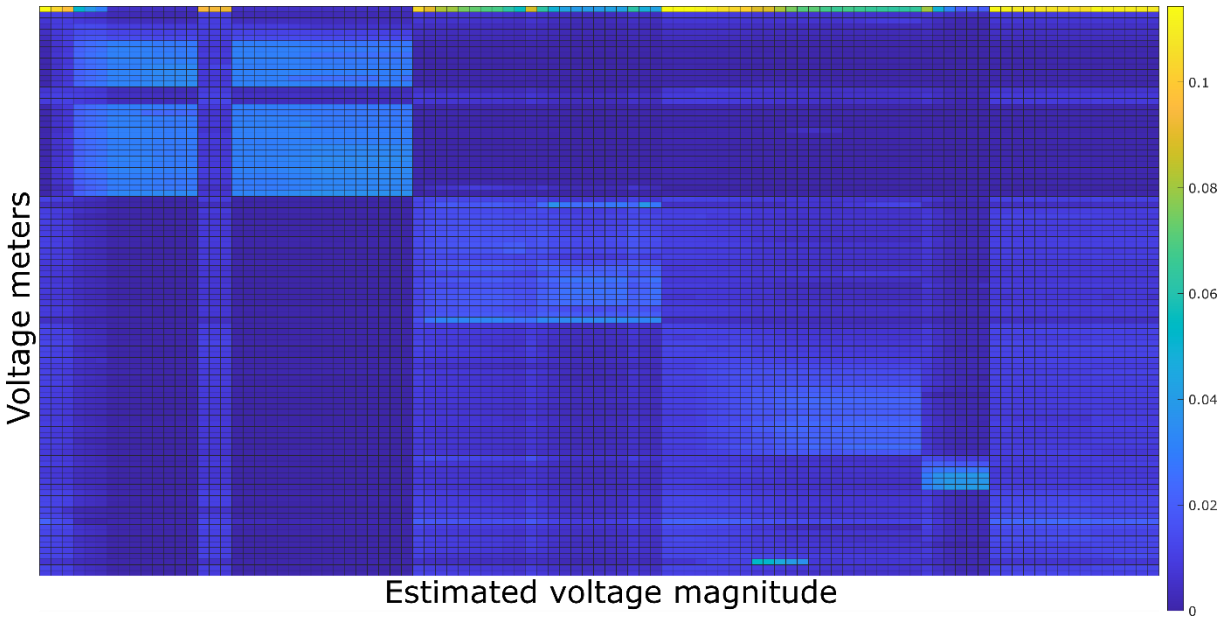

Figure 36. Heatmap for voltage meters – UV case.

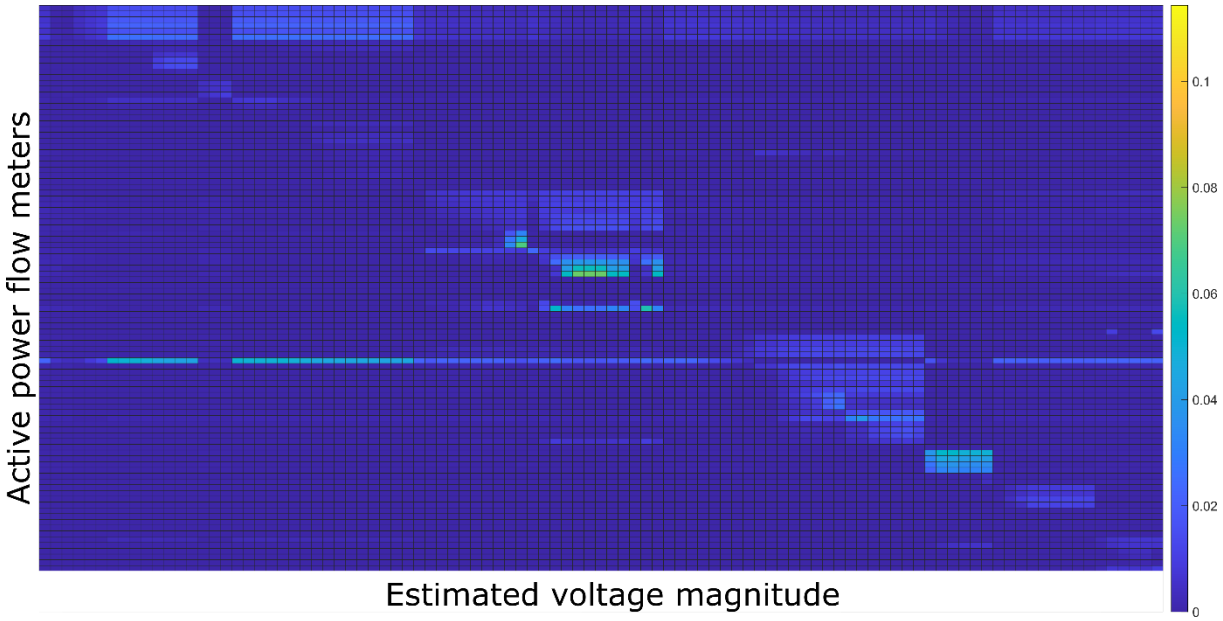

Figure 37. Heatmap for active power flow meters – UV case.

Table 6 shows the chosen meters for each of the three proposed ranking metrics combining the results of the OV and UV cases, for this case a threshold of 1% was used. It is worth noting that given the initial uncertainty profiles for the OV and UV cases, the OV case is expected to dominate the ranking since the square of the uncertainties is used as weight. It can also be seen that again the weighted sum with threshold stops suggesting meters once the uncertainty profile falls below the selected threshold and that the three metrics have the same first three suggestions, however, this is not always the expected

behavior. Figure 38 and Figure 39, Figure 40 and Figure 41, and Figure 42 and Figure 43 show how the uncertainty profiles change with the addition of each of the meters in the list for the "weighted sum", the "weighted sum with threshold" and the "weighted sum for one feeder" metrics, respectively. Analyzing Figure 40 and Figure 41 it can be seen that for the second metric, the uncertainty profile in the UV case falls below the threshold, 1%, after three meters, making the following steps entirely dependent on the OV case.

Table 6. First ten meters suggested by the three metrics.

Weighted sum	Weighted sum with threshold ($\boldsymbol{Thr = 1\%}$)	Weighted sum for one feeder
V32	*V32*	*V32*
V84	*V84*	*V84*
V50	*V50*	*V50*
Pf 62-63	*Pf 62-63*	*V93*
V93	*V93*	*Pf 1-59*
V14	*V6*	*V77*
Pf 35-44	-	*Pf 62-63*
V75	-	*V20*
Pf 1-85	-	*Pf 35-44*
V55	-	*V30*

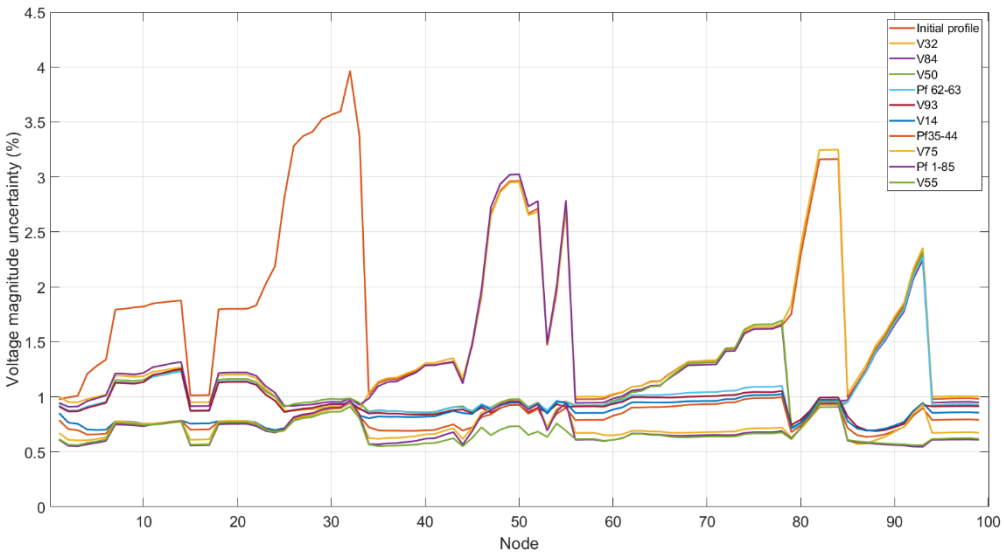

Figure 38. Uncertainty profiles for OV case – weighted sum.

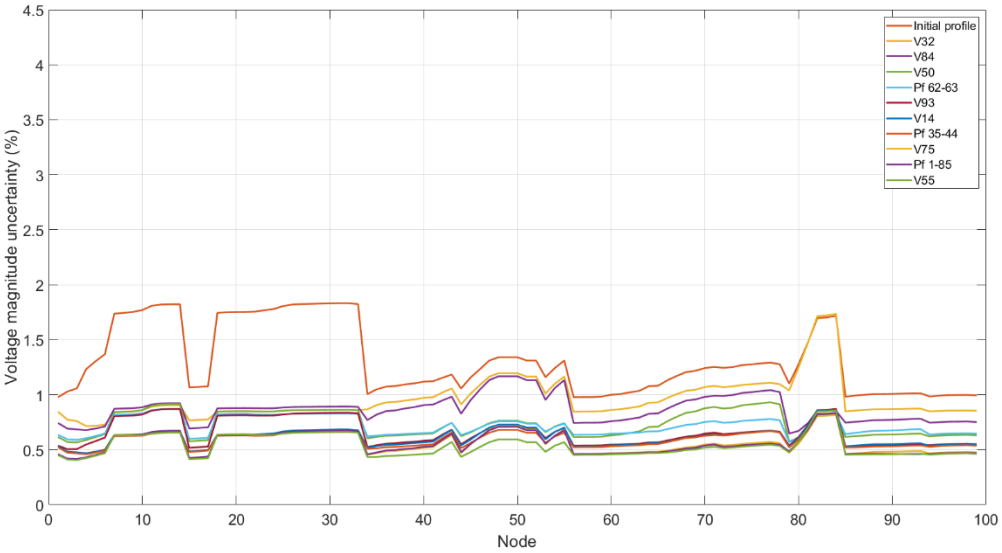

Figure 39. Uncertainty profiles for UV case – weighted sum.

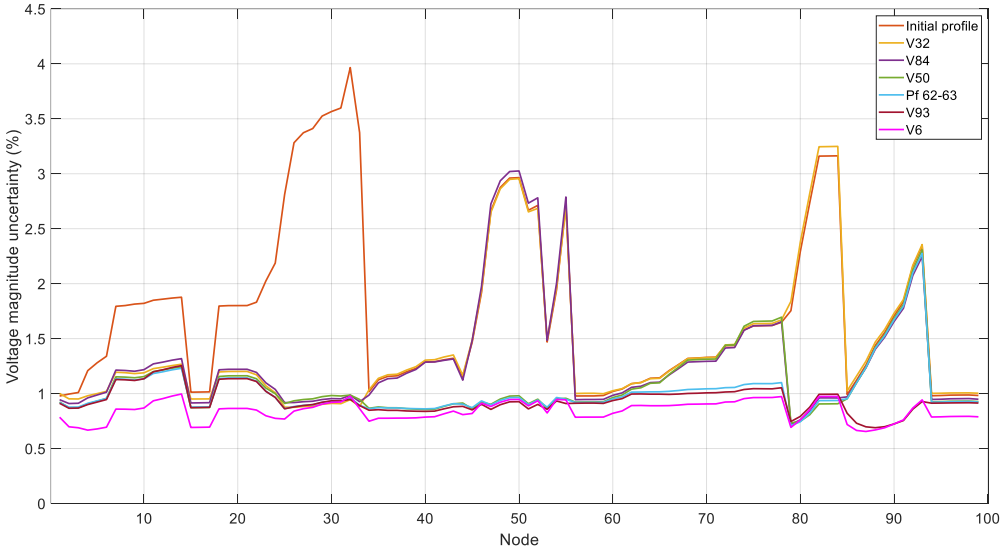

Figure 40. Uncertainty profiles for OV case – weighted sum with threshold.

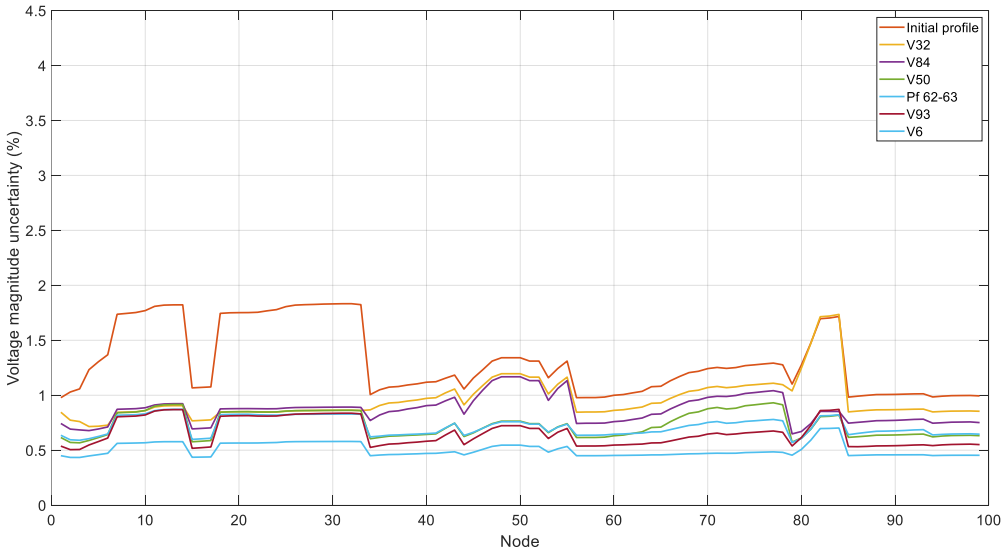

Figure 41. Uncertainty profiles for UV case – weighted sum with threshold.

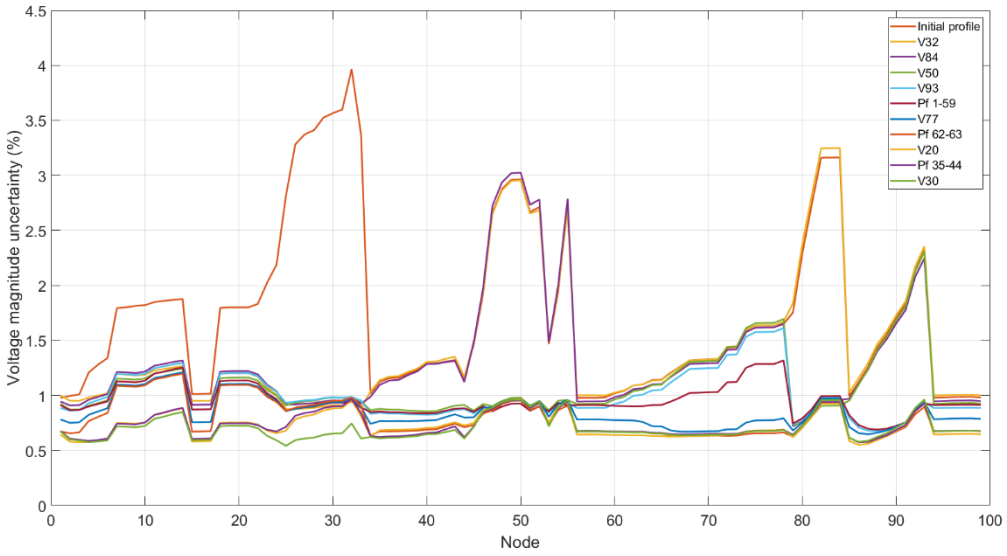

Figure 42. Uncertainty profiles for OV case – weighted sum for one feeder.

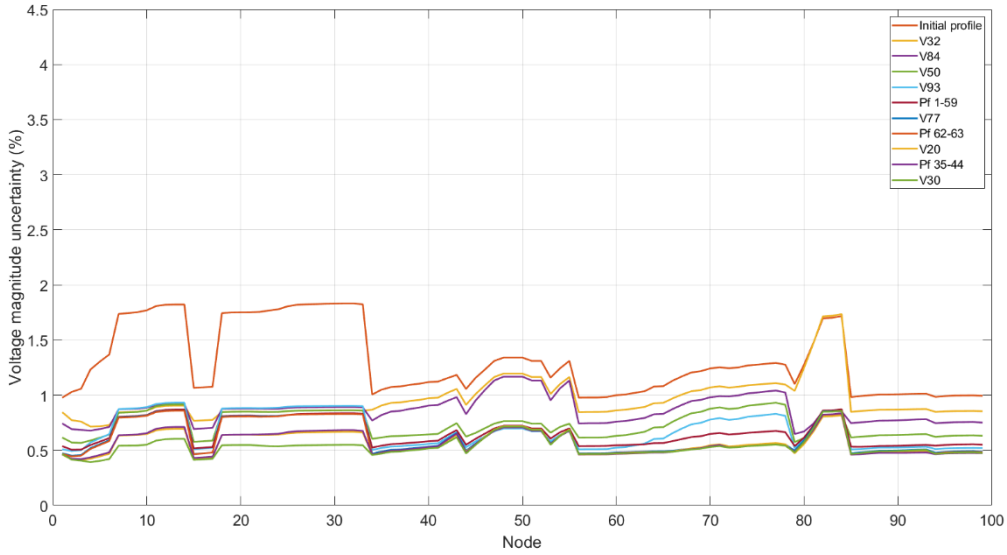

Figure 43. Uncertainty profiles for UV case – weighted sum for one feeder.

If we compare the results obtained for just the OV case with the ones obtained for the combined OV and UV cases, it is visible that in fact, the OV case is dominant, see for example the inclusion of a voltmeter at node 93 which is completely a suggestion from the OV case, since the uncertainty around node 93 is quite low in the UV case. Although not very differentiating, the UV case does have an impact on the final list of meters, this can be seen in the different order of the lists and in the differences in meters recommended that are very similar. For example, in the single OV case the meter V49 is recommended as second for the weighted sum, whereas in the combined case, the meter V50 is recommended as third for the weighted sum. These two meters have almost the same impact in the uncertainty profile, as can be seen in Figure 44, where a large zoom in the plot would be required to appreciate any visual difference between just the effects of each of the meters.

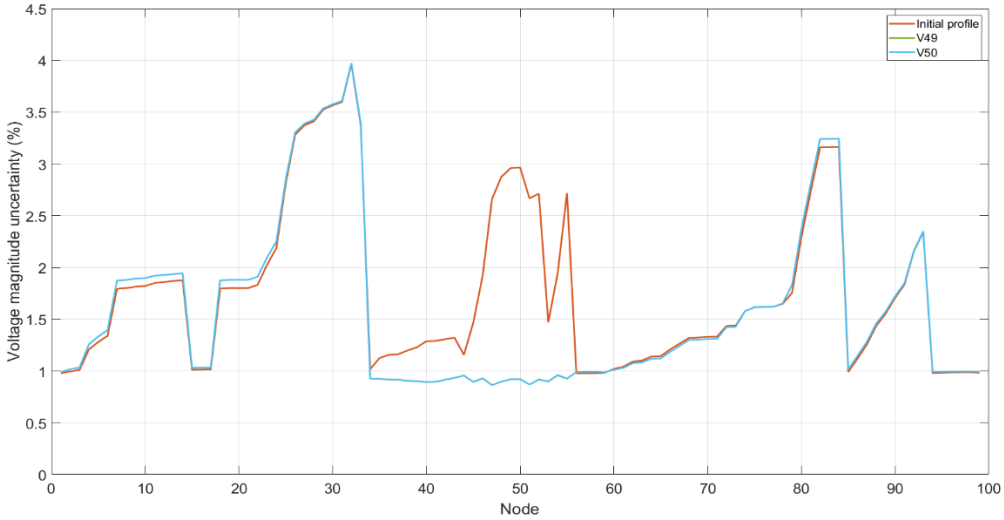

Figure 44. Uncertainty profiles after installing either meter V49 or V50.

4.1.4 OV case for a different year

Considering the connection between the meter placement and the Cost-Benefit analysis, it is worth choosing another year for the simulations to observe differences in the load and generation levels, penetration of renewables, and the extent of overvoltages, for this the year 2018 was chosen. For this scenario we also focus only on the worst OV case, the meter configuration is the same as assumed in the previous cases. Figure 45 shows the initial uncertainty profile for this year and Figure 46 and Figure 47 show the first round heatmaps, again, the heatmaps were divided into only voltage and active power flow meters for visualization purposes, and because the other meters were not as important. For this scenario only the weighted sum was used as ranking metric, Table 7 shows the suggested 10 meters, and Figure 48 shows how the uncertainty profile changes with the addition of each meter. Comparing this scenario with the previous ones, we can see that the initial uncertainty profile is lower than the previous ones, the highest uncertainty being 2.72% in this one, and 3.96% in the others. Another notable thing is that some of the suggested meters are the same as those suggested in previous sections, *V32, V84, V50/V49, Pf 62-63, and V93.*

Table 7. First ten meters suggested by the weighted sum.

Weighted sum
V84
V32
Pf 62-63
V50
Pf 5-6
V93
Pf 1-79
Pf 47-48
Pf 46-54
Pf 47-51

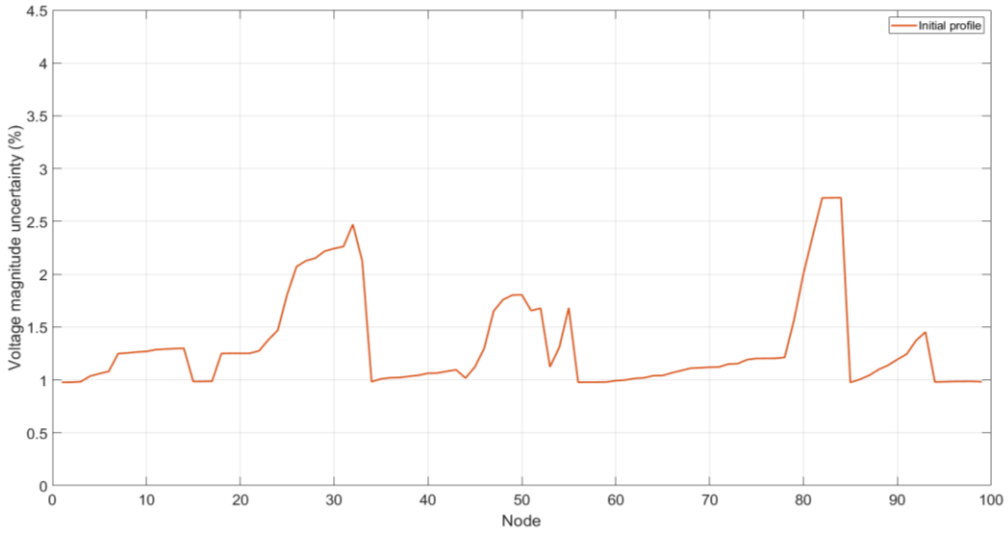

Figure 45. Initial uncertainty profile – OV case 2018.

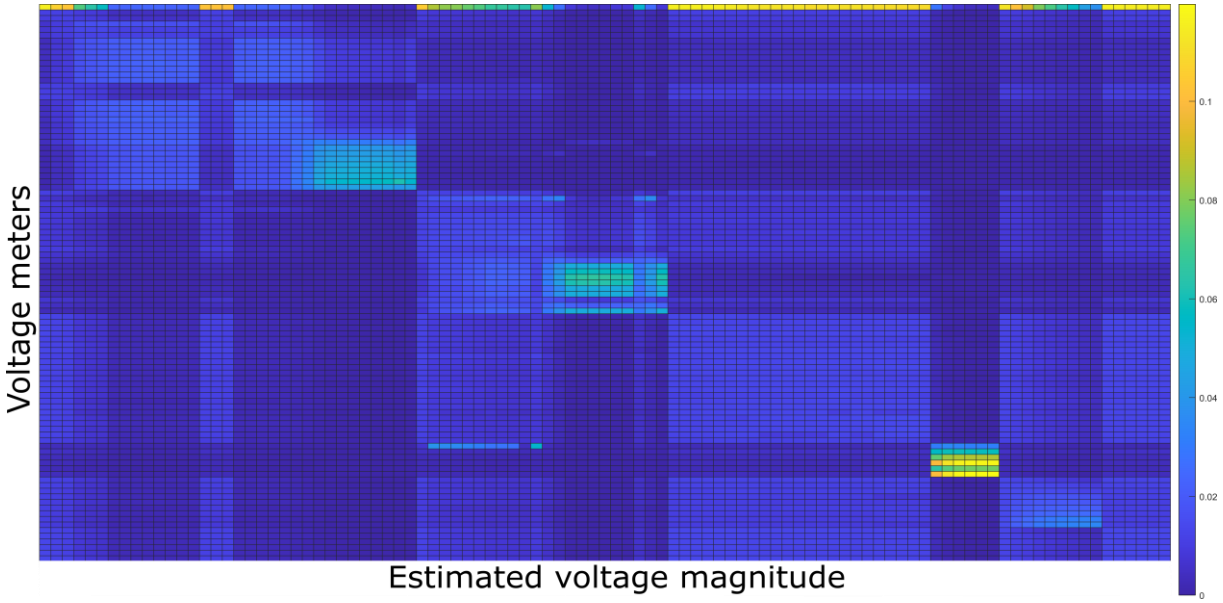

Figure 46. Heatmap for voltage meters – OV case 2018.

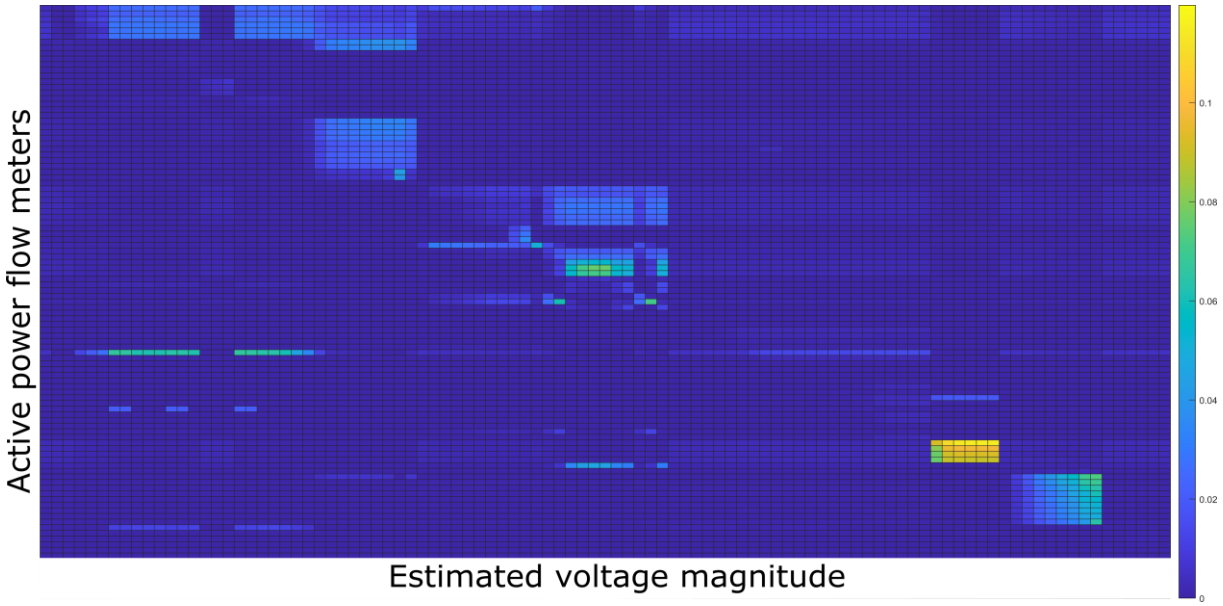

Figure 47. Heatmap for power flow meters – OV case 2018.

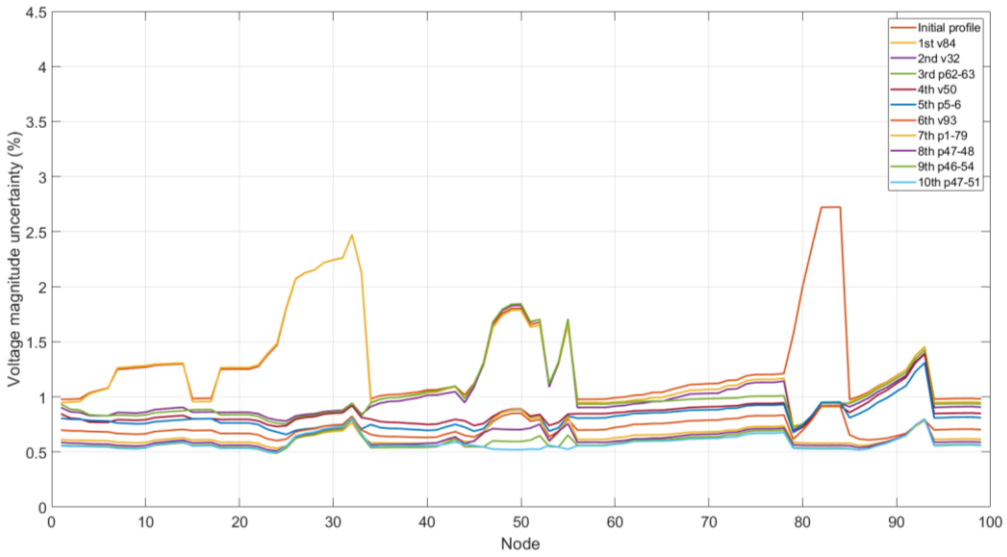

Figure 48. Uncertainty profiles for OV case 2018.

4.2 Cost-benefit analysis results

Having obtained various results from the different scenarios analyzed for the meter placement strategy we can now run simulations for the Cost-Benefit analysis. Using as input the lists of meters obtained, we can then run the CBA routine and see how many meters it makes sense to install in each case, from a cost perspective. A total of eight cases are analyzed in this section, from the single OV case we consider the results obtained using the “weighted sum”, “weighted sum with threshold”, “weighted sum for one feeder” and “modified weighted sum for one feeder” metrics from Section 4.1.2, and the results obtained using the “weighted sum” metric from Section 4.1.4. From the combined OV and UV cases, we consider the results obtained using the “weighted sum”, “weighted sum with threshold” and “weighted sum for one feeder” metrics from Section 4.1.3.

Before performing the Cost-Benefit analysis we need to establish the cost of flexible power and the cost of meters. The cost of flexible energy was assumed to be 100€/MWh, for positive and negative control power, and only applicable to active power changes. The cost was selected as in [28] and is even a conservative cost considering the cost of balancing energy reported in [29]. A reference cost for reactive power provision was not found in accessible sources, moreover, a remuneration for generators providing this service is not common in electricity markets. Belgium was found to be the only European country to incorporate a market for reactive power [30, 31], but its prices are not publicly available [32]. The yearly cost of the meters was assumed to be the same for all types of meters and to be 40,000€ distributed over 15 years or 2,666€/yr, based on meter costs reported in [33]. Another input that must be defined is the initial meter configuration, in this case, is the same configuration used for the meter placement scenarios: one voltmeter at node 1, with 1% uncertainty, and power injection pseudo-measurements at all nodes, except node 1, with 50% uncertainty.

It is worth noting that even though the costs, and the list of meters used, are key factors in the decision-making process of the Cost-Benefit Analysis, the really important part is how they are used in the framework of the Cost-benefit analysis, and that they are just inputs to the analysis that can, and should, be adjusted to fit the circumstances of any future user of the proposed framework. Additionally, it is also possible to obtain the list of meters under consideration from any other meter placement strategy without any impact on the Cost-Benefit analysis.

Table 8 shows a summary of the results of the Cost-Benefit Analysis, each row represents one of the scenarios mentioned earlier, where the 1st metric is the “weighted sum”, the 2nd metric is the “weighted sum with threshold”, the 3rd metric is the “weighted sum for one feeder”, and the modified 3rd metric is the “modified weighted sum for one feeder”. The initial yearly cost for the 2030 scenarios is not available because, with the initial meter configuration in these scenarios, there was a time step where the uncertainty of an estimated magnitude surpassed the 5% limit, the value given in the table was calculated by forcing the uncertainty to be 4.98% at those time steps which emulates an attempt at correcting the voltages as much as possible.

Table 8. Summary of the Cost-Benefit Analysis results.

	Scenario	Number of meters installed	Initial yearly cost (€/yr)	Final yearly cost (€/yr)
2030	1st metric – OV	4	≈253,747	82,449
	2nd metric – OV	3	≈253,747	86,903
	3rd metric – OV	4	≈253,747	82,371
	Modified 3rd metric – OV	2	≈253,747	90,079
	1st metric – UV+OV	3	≈253,747	86,926
	2nd metric – UV+OV	3	≈253,747	86,926
	3rd metric – UV+OV	4	≈253,747	82,447
2018	1st metric – OV	2	79,048	15,908

Two things to notice are the differences in magnitudes of the costs for the 2018 and 2030 scenarios, where the initial cost for the former is still lower than the final cost for the latter, and how with just

two meters a big cost improvement can be made. This shows how much the results of the Cost-Benefit analysis are influenced by the operating conditions. For the 2018 case, having lower load and generation levels, and voltage uncertainties, with only two meters the total costs were reduced by a factor of almost five, whereas for the 2030 scenarios the biggest reduction factor, for the metrics going up to the fourth meter, was about 3.

Another thing to notice is how similar the results of all the metrics are. This is due to the fact that the meter placement results are anyway very similar, in fact, the first 4 suggested meters are the same for the scenarios that reach the 4 meters installed, and even if the suggested fifth meter changes from *Pf 62-63* to *Pf 1-59* when we compare the 1st metric with the 3rd one, both of the meters act to reduce the uncertainty on the same feeder. Moreover, one of these two meters is the meter that makes the CBA procedure stop in all of the cases, if we look at the voltage magnitudes and the restricted voltage limits during the year for the nodes in the feeder on which these meters act, we see that the voltages are never outside the restricted limits. The installation of any of these two meters then makes no difference in the output of the voltage control algorithm, i.e., the requested flexible power by the voltage control, and its associated cost, are the same with or without these meters present in the grid, since the voltages do not need to be corrected.

Figure 49 shows how the savings due to the installation of each additional meter change at every iteration of the Cost-Benefit analysis loop for the simulated scenarios. The dashed line represents the yearly cost of each meter, which is always constant, and the other bars represent the savings, the difference between the cost of flexible power from the previous round, and the cost with the meter under consideration for each scenario. When the bar for any of the scenarios is below the dashed line it means that the currently considered meter is more expensive than the savings due to its installation and the CBA procedure stops. The first bars of all the scenarios were trimmed for visualization purposes, the value for the 2030 scenarios is 157,639 €/yr and for the 2018 scenario is 59,327 €/yr. The first bars of the other scenarios were calculated using the assumed initial cost shown in Table 8. Figure 50 shows the final total cost of each scenario, composed of the total cost of the meters installed (in red), and the cost of the flexible power considering all the meters installed (in blue).

Figure 51 shows how the total cost evolves for each scenario as each new meter is installed and, also shows what the total cost is at the meter that stops the Cost-Benefit analysis loop, the first bars of the 2030 scenarios are the assumed initial cost shown in Table 8, since with the initial meter configuration the year simulation could not be done. This figure was also trimmed for visualization purposes. From this figure, it can be seen how the cost of flexible power does not change when the considered meter is *Pf 62-63* or *Pf 1-59*, as explained previously.

Looking at the results for metric 2, it can be seen that in the combined OV+UV case it has the same results as metric 1, even though the suggested meters are not all the same. It can also be seen that the fact that the meter placement done with metric 2 and 1% as threshold only goes for 7 rounds doesn't affect the result of the CBA in this case, since the Cost-Benefit Analysis indicates that only the first 3 meters make sense to be installed. If instead, the CBA had stopped at the 7th meter, then the meter placement should have been continued with a lower threshold and then incorporate the additional

meters into the Cost-Benefit Analysis, although the originally suggested meters are not guaranteed to be the same as if the meter placement were done with the lower threshold from the beginning.

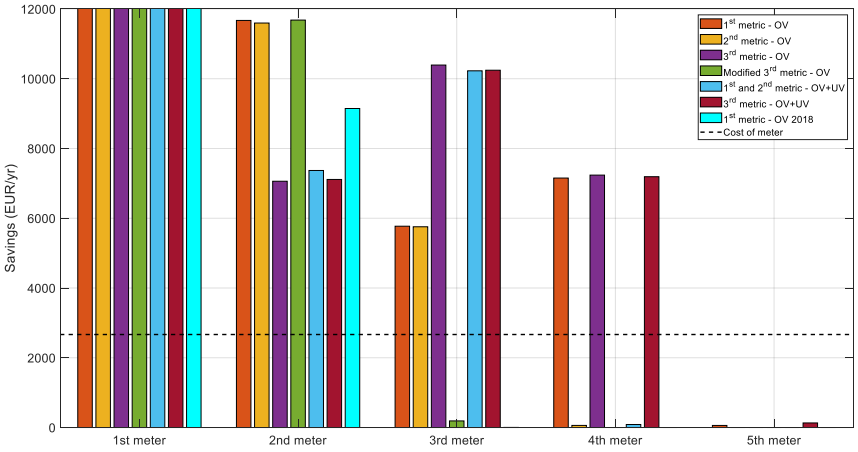

Figure 49. Cost of meter vs savings for the different scenarios.

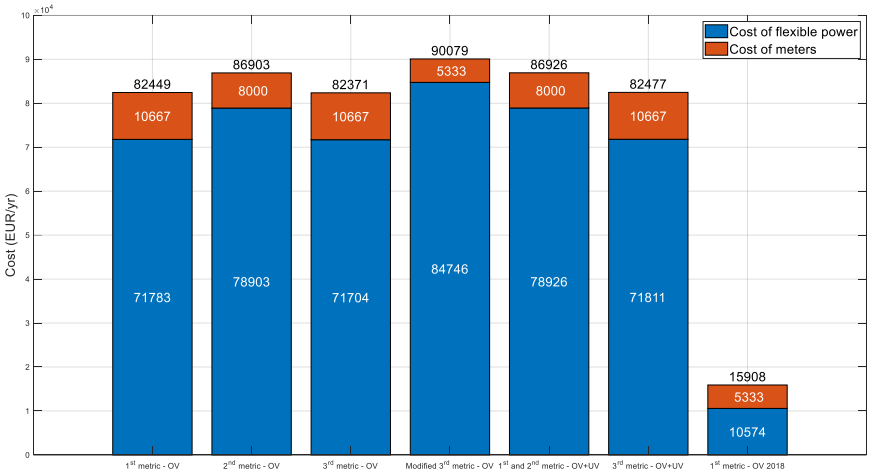

Figure 50. Final total cost for the different scenarios.

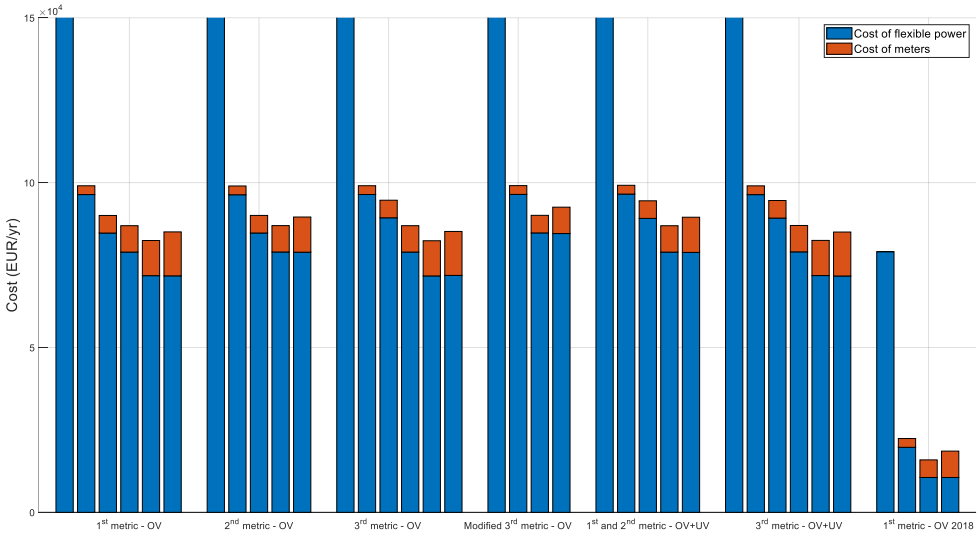

Figure 51. Total cost at each iteration for the different scenarios.

5 Conclusions and Future Work

Considering the main goals of this thesis, an innovative cost-benefit analysis framework for the installation of meters in distribution grids was proposed. Firstly, a new approach to the meter placement problem in distribution networks is proposed by making use of variance-based GSA, showcasing its applicability and versatility in multiple power system applications. The proposed meter placement focuses on the installation of meters that would bring a significant reduction to the uncertainty profile of the voltage magnitude estimates, in a way that depends on the ranking metric used, rather than on finding the minimum meter configuration that brings the uncertainty of the estimates below a given threshold. Secondly, a cost comparison framework was established to evaluate the installation of a new meter in the grid from a cost perspective by considering the savings brought by the meter in terms of voltage control-related costs. These two main parts of the work were then paired under a coupled workflow where the results of the meter placement were then used as inputs for the cost-benefit analysis to evaluate from a cost perspective the viability of the proposed meter placement.

A key characteristic of the software implementation is its modularity, making its two parts completely independent. Any of the two parts could be exchanged or extracted from the proposed implementation for different purposes, the GSA-based meter placement can be replaced by any other meter placement technique without affecting the cost-benefit analysis, or the cost-benefit analysis can be removed to use the meter placement for any other SE-based application.

Chapter 3 explains the proposed workflow implementation and how the two main parts work. The meter placement strategy explanation shows the necessary pre-steps to apply GSA, showing how much the uncertainties of the GSA inputs can affect the results of the meter placement, too much uncertainty can underestimate the effect of meters and too little can overestimate it. Although the selection of these uncertainties is very grid dependent and a standard way of doing this is not proposed, general guidelines are presented in this regard. The framework for the Cost-Benefit analysis is also presented, showing the integration of the voltage control algorithm and how simulations for a year are set up and run in order to compare the yearly cost of the meters with the cost of the yearly flexible power used for voltage control.

Chapter 4 presents the simulation results for the 99-node industrial grid. The results for the meter placement strategy allow us to conclude that the placement is affected when considering different generation and load levels, and DER penetration, as in the 2030 scenarios where the costs were higher than in the 2018 scenario. Although the specific meter selection varies, the three proposed ranking metrics are shown to have very similar results, showing that different meters can have similar impacts on the uncertainty profile. As an additional advantage of the proposed strategy, it can be noted that different ranking metrics can be used to make the meter placement fit different objectives without changing the GSA setup. The obtained results prove how the choice of a proper metric for the application under analysis is crucial, as differences can still be found depending on the implemented metric.

The use of different operating conditions has a great influence on the uncertainty of the state estimation, being able to make some uncertainties rise or fall considerably, which results in the scenario with higher uncertainties dominating the results when different scenarios are analyzed together. It is also concluded that the performance of the metrics for the meter placement cannot be completely judged until the CBA is performed, considering that the CBA is the final goal of the whole framework. Comparing the metrics, metrics 1 and 3 are better suited for the CBA than metric 2 since metrics 1 and 3 allow to continue the meter placement until the CBA finds a meter that should not be installed. Metric 2 on the other hand can make the CBA stop if the uncertainty profile falls below the chosen threshold and the CBA has not found a meter that should not be installed, in which case a lower threshold can be selected and continue the CBA or the whole process could be restarted with the lower threshold.

The results of the CBA show how much the CBA is influenced by the results of the meter placement. It can also be concluded that, contrary to what one would think, a high number of meters is not necessary to achieve relatively large savings, especially in cases with low generation, load, and DER levels. Because of the way that the CBA is proposed, the considered costs for meters and power are also of great influence in the CBA results, however, this was thought as an intended characteristic since costs of power and meters might be very location-dependent and it makes the framework applicable for any DSO. The modularity of the framework implementation also allows us to use the meter placement strategy for other SE-based applications, or the cost-benefit analysis together with other similar meter placement strategies.

In conclusion, a new Cost-Benefit analysis framework for the installation of meters in distribution grids has been proposed to help DSOs in their decision-making process, showcasing the applicability of GSA techniques for this specific power system applications and making use of a robust voltage control strategy for current and future power systems with high DER penetration. The proposed approach connects the meter placement strategy with a grid management task as is the voltage control, making the decision on whether to install a meter dependent on the economic benefits that the installation of the meter could bring, from the voltage control perspective and not just on whether or not the estimation uncertainties are below a given threshold.

5.1 Future work

Regarding the meter placement strategy, some variations can be made to add more degrees of freedom for the analysts/DSOs, for example, by considering PMUs as potential meters, or to expand or improve the capabilities of the meter placement, the use of different GSA techniques (Borgonovo, Morris, HDMR, PAWN) can be used to obtain improvements in terms of computational time and meter selection, for example by using screening techniques to reduce the dimensionality of the problem by eliminating nonimportant inputs. New metrics can be proposed and explored to improve the meter selection or to better adapt to different analysis purposes. Since the meter placement strategy in its core is a way of improving the State Estimation, it could also be expanded to other SE-based applications.

Some extensions to the Cost-Benefit analysis can be in the consideration of different costs for different types of meters, as well as considering the possible dependency of the meter cost on the location in which they are to be installed. Regarding the costs of flexible power, the inclusion of costs associated with the provision of reactive power can be considered, as well as time-based costs for power, since the energy prices fluctuate during the day, especially if high-resolution load and generation profiles are available.

6 References

[1] M. Ginocchi, F. Ponci, and A. Monti, “Sensitivity Analysis and Power Systems: Can We Bridge the Gap? A Review and a Guide to Getting Started,” *Energies*, vol. 14, no. 24, p. 8274, 2021, doi: 10.3390/en14248274.

[2] M. Pau, E. de Din, F. Ponci, P. A. Pegoraro, S. Sulis, and C. Muscas, “Impact of uncertainty sources on the voltage control of active distribution grids,” in *2021 International Conference on Smart Energy Systems and Technologies (SEST)*, Vaasa, Finland, 2021, pp. 1–6.

[3] M. Pau, P. A. Pegoraro, S. Sulis, and C. Muscas, “Uncertainty sources affecting voltage profile in Distribution System State Estimation,” in *2015 IEEE International Instrumentation and Measurement Technology Conference (I2MTC) Proceedings*, Pisa, Italy, 2015, pp. 109–114.

[4] M. Pau, F. Ponci, and A. Monti, “Impact of Network Parameters Uncertainties on Distribution Grid Power Flow,” in *2019 International Conference on Smart Energy Systems and Technologies (SEST)*, Porto, Portugal, 2019, pp. 1–6.

[5] R. Minguez and A. J. Conejo, “State Estimation Sensitivity Analysis,” in *MELECON 2006 - 2006 IEEE Mediterranean Electrotechnical Conference*, Benalmadena, Spain, 2006, pp. 956–959.

[6] T. Stuart and C. Herczet, “A Sensitivity Analysis of Weighted Least Squares State Estimation for Power Systems,” *IEEE Trans. on Power Apparatus and Syst.*, PAS-92, no. 5, pp. 1696–1701, 1973, doi: 10.1109/TPAS.1973.293718.

[7] A. Ahmadifar, M. Ginocchi, M. S. Golla, F. Ponci, and A. Monti, “Development of an Energy Management System for a Renewable Energy Community and Performance Analysis via Global Sensitivity Analysis,” *IEEE ACCESS*, vol. 11, pp. 4131–4154, 2023, doi: 10.1109/access.2023.3235590.

[8] A. Dognini, M. Ginocchi, E. de Din, F. Ponci, and A. Monti, “Service Restoration of AC–DC Distribution Grids Based on Multiple-Criteria Decision Analysis,” *IEEE ACCESS*, vol. 11, pp. 15725–15749, 2023, doi: 10.1109/ACCESS.2023.3244872.

[9] R. Scalabrin and G. Cocchi, “Sensitivity Analysis of a State Estimator and State Estimation based Applications,” Master thesis, Scuola di ingegneria industriale e dell'informazione, Politecnico Milano, 2022.

[10] M. E. Baran, J. Zhu, and A. W. Kelley, “Meter placement for real-time monitoring of distribution feeders,” *IEEE Trans. Power Syst.*, vol. 11, no. 1, pp. 332–337, 1996, doi: 10.1109/59.486114.

[11] M. Ghasemi Damavandi, V. Krishnamurthy, and J. R. Marti, “Robust Meter Placement for State Estimation in Active Distribution Systems,” *IEEE Trans. Smart Grid*, vol. 6, no. 4, pp. 1972–1982, 2015, doi: 10.1109/TSG.2015.2394361.

[12] J. Liu, F. Ponci, A. Monti, C. Muscas, P. A. Pegoraro, and S. Sulis, “Optimal Meter Placement for Robust Measurement Systems in Active Distribution Grids,” *IEEE Trans. Instrum. Meas.*, vol. 63, no. 5, pp. 1096–1105, 2014, doi: 10.1109/TIM.2013.2295657.

[13] N. Nusrat, M. Irving, and G. Taylor, “Novel meter placement algorithm for enhanced accuracy of distribution system state estimation,” in *2012 IEEE Power and Energy Society General Meeting*, San Diego, CA, 2012, pp. 1–8.

[14] R. Singh, B. C. Pal, R. A. Jabr, and R. B. Vinter, “Meter Placement for Distribution System State Estimation: An Ordinal Optimization Approach,” *IEEE Trans. Power Syst.*, vol. 26, no. 4, pp. 2328–2335, 2011, doi: 10.1109/TPWRS.2011.2118771.

[15] E. Zio, *The Monte Carlo simulation method for system reliability and risk analysis*. London: Springer, 2013.

[16] I. Sobol’, “Global sensitivity indices for nonlinear mathematical models and their Monte Carlo estimates,” *Mathematics and Computers in Simulation*, vol. 55, 1-3, pp. 271–280, 2001, doi: 10.1016/S0378-4754(00)00270-6.

[17] B. Sudret, “Global sensitivity analysis using polynomial chaos expansions,” *Reliability Engineering & System Safety*, vol. 93, no. 7, pp. 964–979, 2008, doi: 10.1016/j.ress.2007.04.002.

[18] A. Saltelli, “Making best use of model evaluations to compute sensitivity indices,” *Computer Physics Communications*, vol. 145, no. 2, pp. 280–297, 2002, doi: 10.1016/S0010-4655(02)00280-1.

[19] Marelli S., Lüthen N., and Sudret B., “UQLab user manual - Polynomial chaos expansions,” Chair of Risk, Safety and Uncertainty Quantification, ETH Zurich,Switzerland, 2022.

[20] G. Blatman, “Adaptive sparse polynomial chaos expansions for uncertainty propagation and sensitivity analysis,” Université Blaise Pascal, Clermont-Ferrand, France, 2009.

[21] Marelli S., Lamas C., Konakli K., Mylonas C., Wiederkehr P., and Sudret B., “UQLab user manual - Sensitivity analysis,” Chair of Risk, Safety and Uncertainty Quantification, ETH Zurich,Switzerland, 2022.

[22] F. Ponci, “Advanced Monitoring for Power Systems: Module I – Course Introduction,” 2022.

[23] F. Pilo *et al.,* “ATLANTIDE - Digital archive of the Italian electric distribution reference networks,” in *CIRED 2012 Workshop: Integration of Renewables into the Distribution Grid*, Lisbon, Portugal, 2012, p. 165.

[24] A. Bracale *et al.,* “Analysis of the Italian distribution system evolution through reference networks,” in *2012 3rd IEEE PES Innovative Smart Grid Technologies Europe (ISGT Europe)*, Berlin, Germany, 2012, pp. 1–8.

[25] G. Celli, F. Pilo, G. Pisano, and G. G. Soma, “Reference scenarios for Active Distribution System according to ATLANTIDE project planning models,” in *2014 IEEE International Energy Conference (ENERGYCON)*, Cavtat, Croatia, 2014, pp. 1190–1196.

[26] S. Marelli and B. Sudret, “UQLab: A Framework for Uncertainty Quantification in Matlab,” in *Vulnerability, Uncertainty, and Risk*, Liverpool, UK, 2014, pp. 2554–2563.

[27] The MathWorks, Inc., *kmedoids.* [Online]. Available: https://www.mathworks.com/help/stats/kmedoids.html (accessed: Sep. 5 2023).

[28] R. Bolgaryn, Z. Wang, A. Scheidler, and M. Braun, “Active Power Curtailment in Power System Planning,” *IEEE Open J. Power Energy*, vol. 8, pp. 399–408, 2021, doi: 10.1109/OAJPE.2021.3118445.

[29] Amprion GmbH, *BALANCING GROUP PRICE.* [Online]. Available: https://www.amprion.net/Energy-Market/Balancing-Groups/Balancing-Group-Price/ (accessed: May 15 2023).

[30] T. Wolgast, S. Ferenz, and A. Niesse, “Reactive Power Markets: A Review,” *IEEE ACCESS*, vol. 10, pp. 28397–28410, 2022, doi: 10.1109/ACCESS.2022.3141235.

[31] SmartNet Consortium, *D1.1: Ancillary Service Provision by RES and DSM Connected at Distribution Level in the Future Power System.* [Online]. Available: https://smartnet-project.eu/publications/index.html#tab-id-2 (accessed: May 15 2023).

[32] Elia, *Open Data Portal.* [Online]. Available: https://opendata.elia.be/explore/?disjunctive.theme&disjunctive.dcat.granularity&disjunctive.dcat.accrualperiodicity&disjunctive.keyword&sort=explore.popularity_score&refine.keyword=Bidding&refine.keyword=Costs (accessed: May 15 2023).

[33] F. G. Duque, L. W. de Oliveira, E. J. de Oliveira, and J. C. de Souza, “A cost-benefit multiobjective approach for placement of meters in electrical distribution systems,” *Electric Power Systems Research*, vol. 191, p. 106897, 2021, doi: 10.1016/j.epsr.2020.106897.